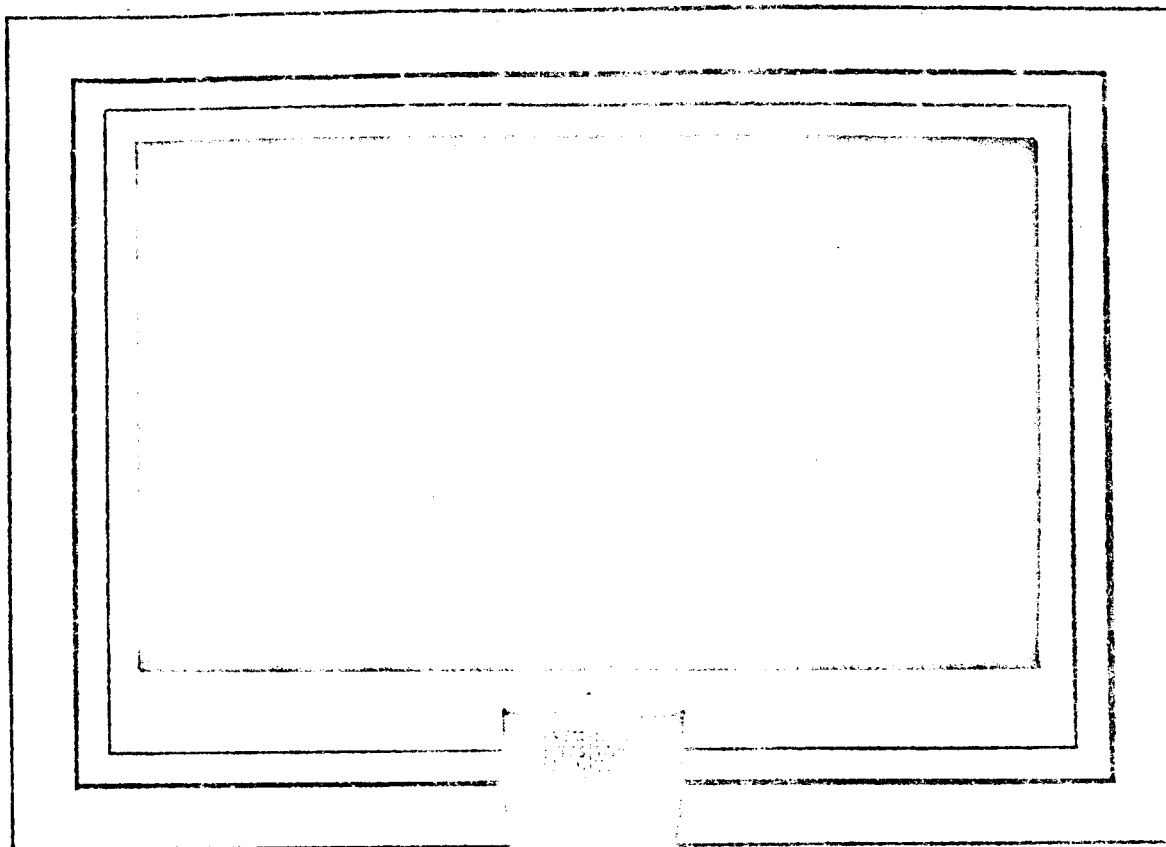


(NASA-CR-157637) THRUST TRANSIENT
PREDICTION AND CONTROL OF SOLID ROCKET
ENGINES (Princeton Univ., N. J.) 73 p

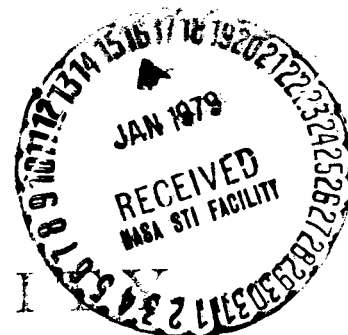
00/20

Unclass
35411

N79-71468



BEST AVAILABLE COPY



PRINCETON UNIVERSITY
DEPARTMENT OF
AEROSPACE AND MECHANICAL SCIENCES

THRUST TRANSIENT PREDICTION AND CONTROL
OF SOLID ROCKET ENGINES

(Presentation Version)

Aerospace and Mechanical Sciences
Report No. 837

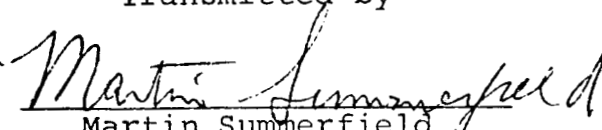
by

W. J. Most, B. W. MacDonald, P. L. Stang
and M. Summerfield

June, 1968

This research was sponsored by the Office of Advanced Research and Technology, National Aeronautics and Space Administration, under NASA Grant NGR 31-001-109.

Transmitted by


Martin Summerfield
Principal Investigator

This report consists of reproductions of slides and motion picture captions presented at the Third ICRPG/AIAA Solid Propulsion Conference, Atlantic City, New Jersey, June 4-6, 1968. Additional copies of this presentation version are available from Princeton University.

Guggenheim Laboratories for the Aerospace Propulsion Sciences
Department of Aerospace & Mechanical Sciences
PRINCETON UNIVERSITY
Princeton, New Jersey

EXPLANATORY NOTE

Presentation Version

This report consists of reproductions of slides and motion picture captions comprising a presentation given at the Third ICRPG/AIAA Solid Propulsion Conference in Atlantic City, New Jersey on June 4-6, 1968. As such it does not include the verbal explanations that accompanied the slides. No manuscript was prepared for the Conference. However, previous publications by the same authors on the subject are available on request. It is hoped that, despite the terseness of this document, it will serve as a useful summary of the new material presented at the Conference. Work on this topic is still continuing and a later report will include revisions of these results along with new results.

TABLE OF CONTENTS

	<u>Page</u>
Title Page	i
Explanatory Note	ii
Table of Contents	iii
Presentation Title Page	iv
I. <u>Introduction</u>	1
A. Review of Previous Literature on the Ignition Transient	3
B. Physical Model of the Ignition Transient	6
C. Sample Theoretical Prediction	19
II. <u>Two-Dimensional Motor Firings Compared With Computer Predictions</u>	20
A. Typical Experimental Run	21
B. Series A - Pressure Overshoots Due to Extended Igniter Duration	25
C. Series B - Effect of Varying the Igniter Duration	28
D. Series C - Effect of Varying Igniter Flow Rate	29
E. Series D - Marginal Igniter Durations	30-A
F. Series E - Effects of Aluminum Addition to Propellant	34-A
III. <u>Application of Prediction Method to Practical Motor Configurations</u>	37
A. Firing Test of Star-Shaped Grain and Theoretical Prediction	39
IV. <u>Conclusions; Problems for Future Work</u>	40
Appendix A: Motion Picture Description of:	43
1. Flame spreading and pressure transient of a two-dimensional rocket motor with an AP propellant grain	56
2. The same as 1 but with an aluminized propellant grain	61
3. The same as 1 but with an undersized igniter, demonstrating slow flame spread (hangfire)	65

THRUST TRANSIENT PREDICTION AND CONTROL
OF SOLID ROCKET ENGINES

W.J. Most
B.W. MacDonald
P.L. Stang
M. Summerfield

Guggenheim Laboratories
Princeton University

Sponsored by NASA
Grant NRG 31-001-109

Supervised by
Langley Research Center

June 4, 1968

This paper will include:

1. Physical model and theory of motor transient.
2. Theory of spreading of flame over propellant.
3. Review of previous work on transient prediction.
4. Predictions of motor transients based on (1) and (2).
5. Motor firings with non-aluminized AP/PBAA propellant and comparison with predictions.

Continued on next page.

6. Hangfires: comparison of tests with predictions.
7. Motor firings with aluminized vs. non-aluminized propellant.
8. Firings with star grains, gas-less igniters, etc.
9. Future problems -- application to more realistic motors.

At the end (10 minutes):

Movies of flame spreading coupled with motor transients.

Theories of Motor Ignition Transient Prediction
Reviewed in the Paper:

1.	Guth and Dubrow	STL	1963 (C)
2.	Fullman and Neilson	UTC	1963 (C)
3.	Von Elbe	ARC	1963
4.	Summerfield, Parker, Wenograd, Most, Stang, diLauro, Lukenas and MacDonald	Princeton	1964, 1966, 1966, 1966, 1966, 1967, 1967, 1967

Page 1 of 3 pages.

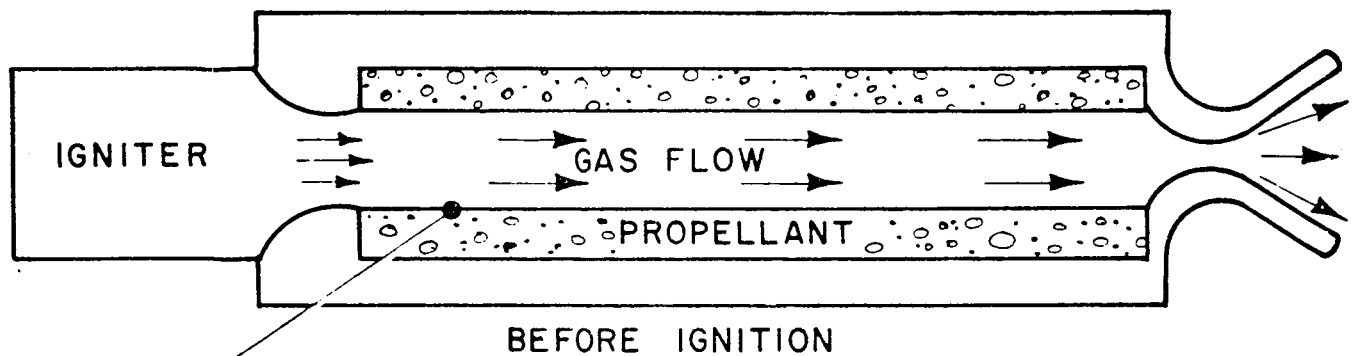
9.	Adams	Thiokol-Huntsville	1965, 1966, 1967
10.	Isom	Hercules	1966
11.	Peleg and Manheimer- Timnat	Technion	1968
12.	Wallis	Imperial Metals Industries, Ltd.	1968

Page 3 of 3 pages.

PAGE 4 INTENTIONALLY BLANK

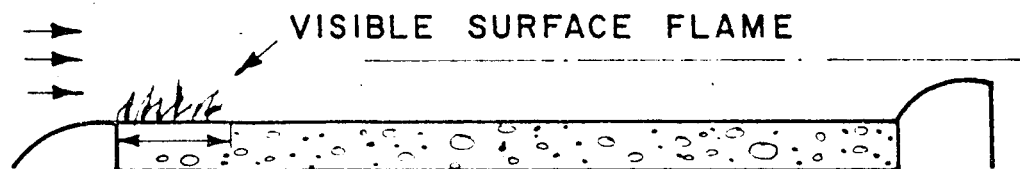
5

SCHEMATIC REPRESENTATION, FLAME SPREADING PHASE OF IGNITION INTERVAL

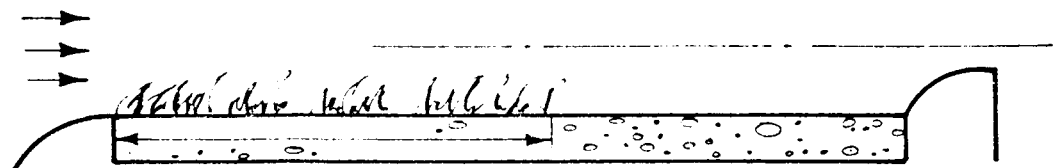


SUCCESSIVE POSITIONS OF SURFACE FLAME
AFTER START OF IGNITION

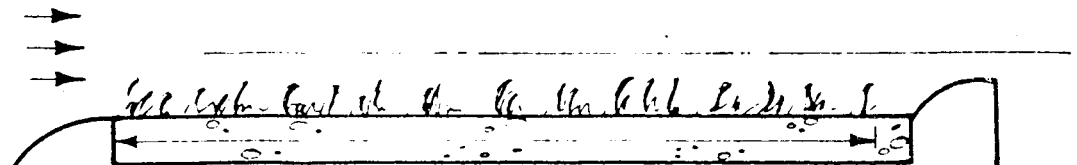
A - FIRST
VISIBLE
FLAME



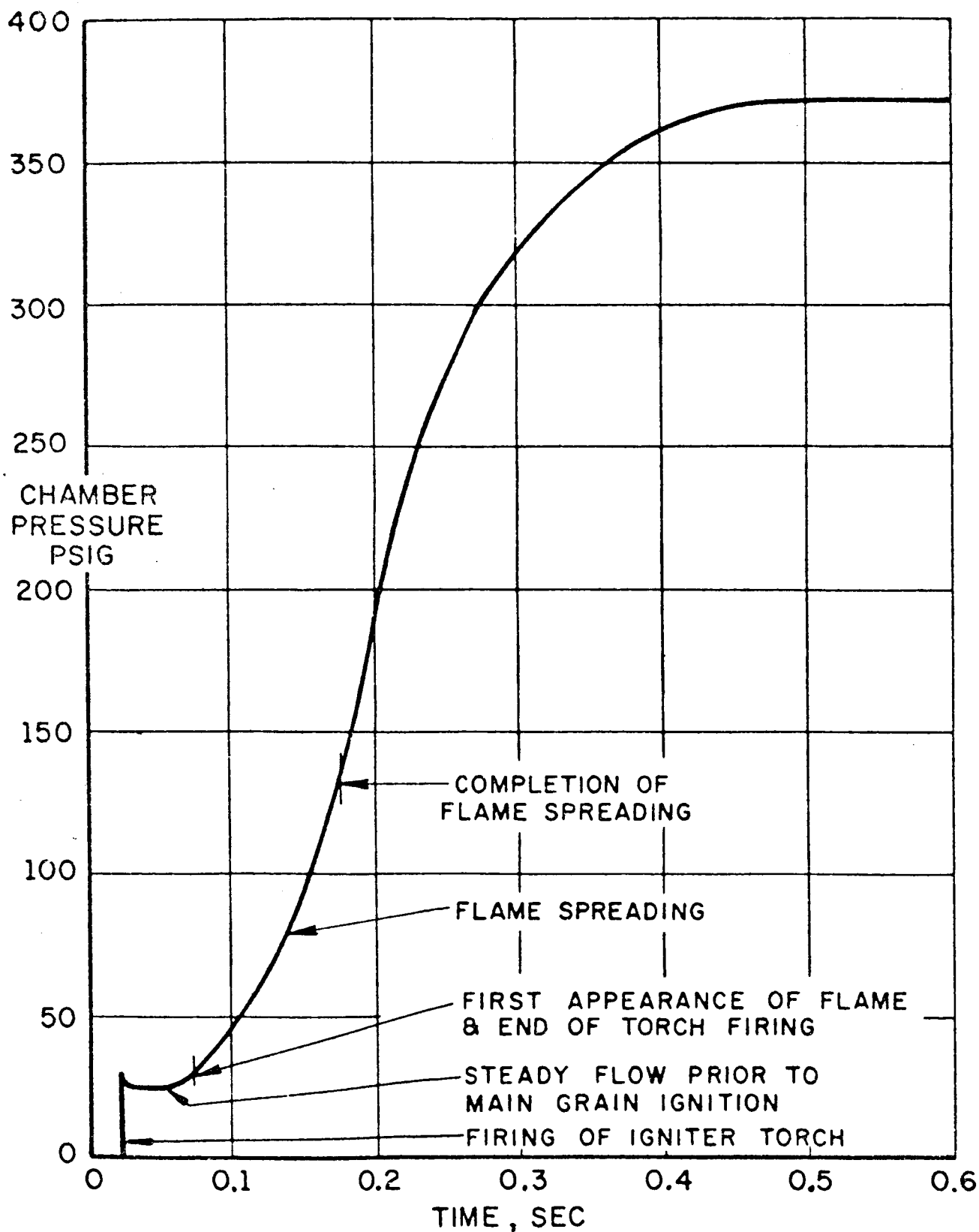
B - INTERMEDIATE
STAGE



C - ALMOST
FULLY
IGNITED



PRESSURE TRANSIENT DURING IGNITION OF TEST MOTOR



MOMENTUM EQUATION

- 1 The port-to-throat area ratio of the rocket motor is large.
- 2 The short nozzle assumption.

$$\Delta p_c = 0$$

CONTINUITY EQUATION

$$\frac{dm_c}{dt} + \dot{m}_N = \dot{m}_B + \dot{m}_{ign}$$

3 The control volume does not vary with time.

$$m_c = \rho_c V_c$$

4 The exhaust nozzle is always choked:

$$\dot{m}_N = \frac{\Gamma p_c A_t}{\sqrt{RT_c}}$$

5 The propellant burning rate is adequately described by a steady state burning rate equation of the form:

$$V_{ss} = k p_c^n \Rightarrow \dot{m}_B = \rho_p S_B(t) r_{ss}$$

6 The perfect gas assumption.

$$\frac{V_c}{R} \frac{d(p_c/T_c)}{dt} + \frac{\Gamma p_c A_t}{\sqrt{RT_c}} - \rho_p S_B r_{ss} - \dot{m}_{ign}(t) = 0$$

ENERGY EQUATION

$$\frac{\partial}{\partial t} \int_V \left(e + \frac{u^2}{2} \right) \rho_c dV_c + \int_S \left(e + \frac{u^2}{2} \right) \rho_c \bar{u} \cdot d\bar{v} \\ = - \int_V p_c \bar{u} \cdot d\bar{v}_c + \left(\text{Heat Addition} \right) + \left(\text{Body Work} \right)$$

- 7 The thickness of the flame is small compared to the dimensions of the control volume.
- 8 The heat addition and body work terms can to neglected.

$$h = e + \frac{u^2}{2}$$

- 9 The igniter gases and the propellant combustion gases are calorically perfect.

$$h = c_p T_c$$

- 10 It was previously assumed that the flow velocity is very low. Therefore, it can be shown that:

$$u^2 \ll h = c_p T_c$$

$$\frac{\partial}{\partial t} \int_V c_p T_c \rho_c dV_c + \int_S c_p T_c \rho_c \bar{u} \cdot d\bar{v}_c - \frac{\partial}{\partial t} \int_V p_c dV = 0$$

$$\underline{1+2} \quad \nabla p_c = 0$$

$$\underline{11} \quad \text{Neglect temperature gradient.} \quad \nabla T_c = 0$$

12 The composition of the igniter gas is the same as the propellant combustion product gas.

$$\frac{d}{dt}(m_c T_c) + \dot{m}_N T_c - \dot{m}_g T_f - \dot{m}_{ign} T_{cign} - \frac{1}{c_p} \frac{d}{dt}(p_c V_c) = 0$$

ENERGY EQUATION

$$\frac{dT_c}{dt} + \int \sqrt{RT_c} A_T T_c (\gamma - 1) - \frac{\rho_p S_B V_{ss}}{\rho_c} RT_c (\gamma T_F - T_c)$$

$$- \frac{RT_c \dot{m}_{ign}}{\rho_c} (\gamma T_{c,ign} - T_c) = 0$$

CONTINUITY EQUATION

$$\frac{V_c}{R} \frac{d}{dt} \left(\frac{\rho_c}{T_c} \right) + \frac{\int \rho_c A_T}{\sqrt{RT_c}} - \rho_p S_B (K \rho^n) - \dot{m}_{ign} = 0$$

NONDIMENSIONAL VARIABLES

$$p = \frac{p_c}{p_{eq}}$$

$$T = \frac{T_c}{T_f}$$

$$T_{cign} = \frac{T_{cign}}{T_f}$$

$$S = \frac{S_B}{A_B}$$

$$\chi = \frac{L}{L^*} = \frac{L}{\left[\frac{L^*}{\Gamma^2 C^*} \right]}$$

$$\dot{m}_{ign} = \frac{\dot{m}_{ign}}{(\dot{m}_N)_{eq}}$$

$$\frac{dp}{dz} = \chi \left[S p^n - \rho T^{1/2} + m_{ign}(z) \right] + (2) m_{ign}(z)$$

$$\frac{dp}{dz} = \frac{I}{I_p} \left[(\chi-1) S p^n - (\chi-1) \rho T^{1/2} + m_{ign}(z) (\chi T_{ign} - T) \right]$$

SOLID PHASE HEAT-UP

$$\rho c_p \frac{\partial T}{\partial t} = \lambda_p \nabla^2 T + \rho c_p \vec{r} \cdot \nabla T + \rho \dot{Q}$$

Simplifying Assumptions:

$$\frac{\partial^2 T}{\partial y^2} \gg \frac{\partial^2 T}{\partial x^2}$$

The convective term is negligible during the ignition interval.

The propellant is completely inert until a critical ignition temperature is reached.

Above the critical surface temperature the burning rate is dictated by the steady state equation,
 $r = ap^n$.

Reduced Equation:

$$\frac{\partial T}{\partial t} = \alpha_p \frac{\partial^2 T}{\partial y^2}$$

(\dot{Q} in the surface region will be re-introduced later.
See page 18.)

Boundary Conditions:

$$T(x, y, 0) = T_0$$

$$T(x, \infty, t) = T_0$$

$$\text{At } y=0 \left(\lambda_p \frac{\partial T}{\partial y} \right)_{y=0} = - \dot{q}_{g=0}(x, t)$$

The heat diffusion equation and the boundary conditions are solved to obtain the propellant surface temperature,

$$T_s = T_0 + \frac{1}{\lambda_p} \sqrt{\frac{\alpha_p}{\pi}} \int_0^t \frac{\dot{q}_g}{\sqrt{t-\tau}} d\tau$$

EQUATIONS FOR HEAT FLUX AT SURFACE

The assumption is made that radiative heat transfer to the propellant grain can be ignored. Only convective heat transfer is considered.

The variation of the boundary layer film coefficient, h , is found from an empirical Nusselt number - Reynolds number correlation.

$$Nu_x = .0734 Re_x^{0.8}$$

$$Nu_x = \frac{hx}{\lambda_g}$$

$$h = .0734 \frac{\lambda_g}{x} Re_x^{0.8}$$

$$\dot{q}_{CONVECTIVE} = h(T_g - T_s)$$

T_g is taken as constant downstream along the motor axis, but varying with time.

SELF HEATING

It was previously assumed that the propellant is completely inert until a critical ignition temperature is reached.

This is an obvious oversimplification. As will be seen later, marginal ignition situations cannot be predicted accurately with this model.

An alternate assumption was tried, that energy is released at the propellant surface while the surface temperature is still below the ignition temperature according to a law:

$$\dot{q}_{\text{SURFACE}} = \rho_p Q A_s e^{\frac{-E_s}{RT_s}}$$

The boundary conditions now become

$$T(x, y, 0) = T_0$$

$$T(x, \infty, t) = T_0$$

$$\text{At } y=0 \left(\lambda_p \frac{\partial T}{\partial y} \right)_{y=0} = -[\dot{q}_{\text{CONV}}(x, t) + \dot{q}_{\text{SURF}}(x, t)]$$

The effect of this self heating term is shown on page 30.

ROCKET MOTOR IGNITION TRANSIENT (THEORETICAL)

SERIES A - FIXED ROCKET GEOMETRY
VARIABLE IGNITER FLOW RATE

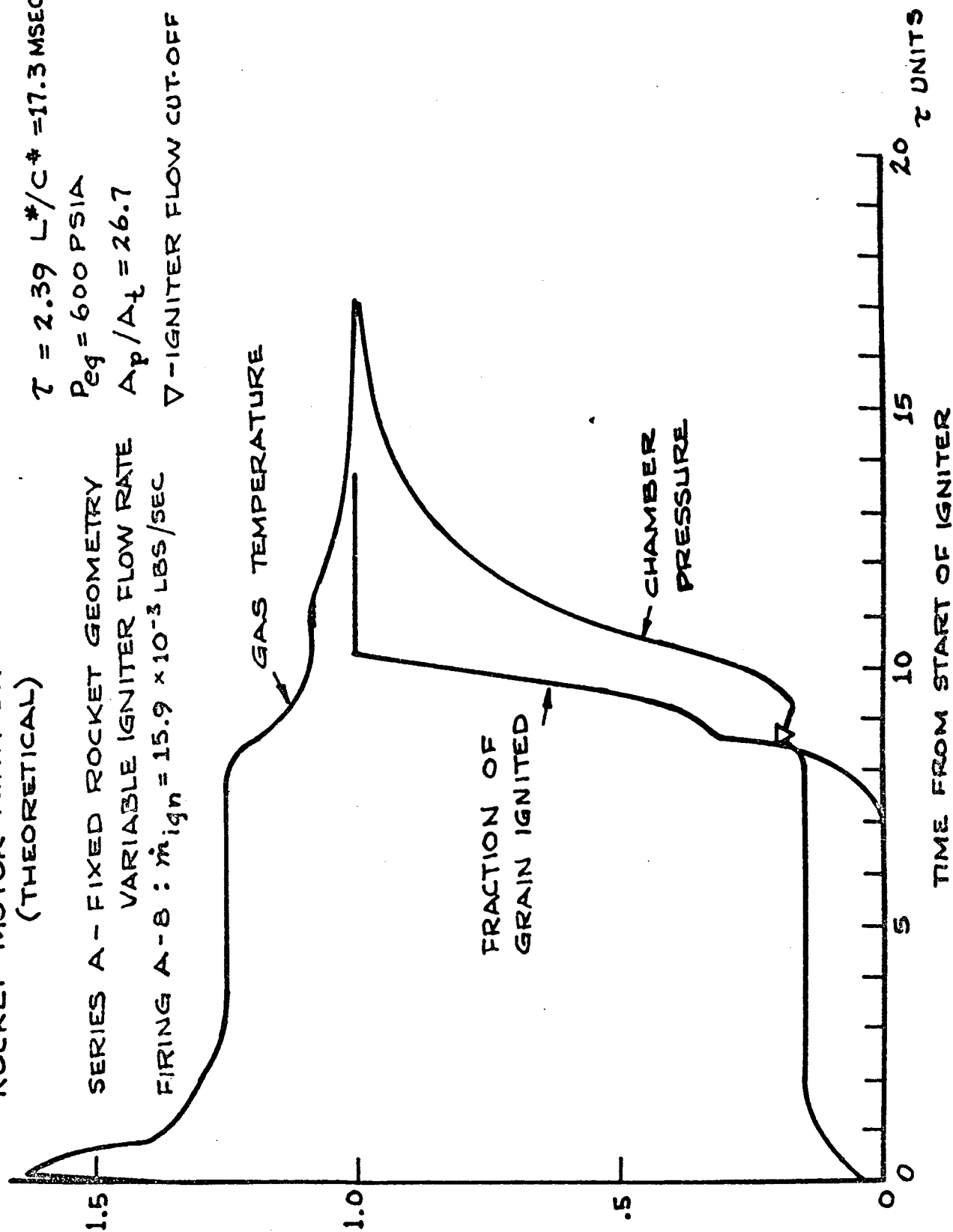
FIRING A-B : $\dot{m}_{ign} = 15.9 \times 10^{-3}$ LBS/SEC

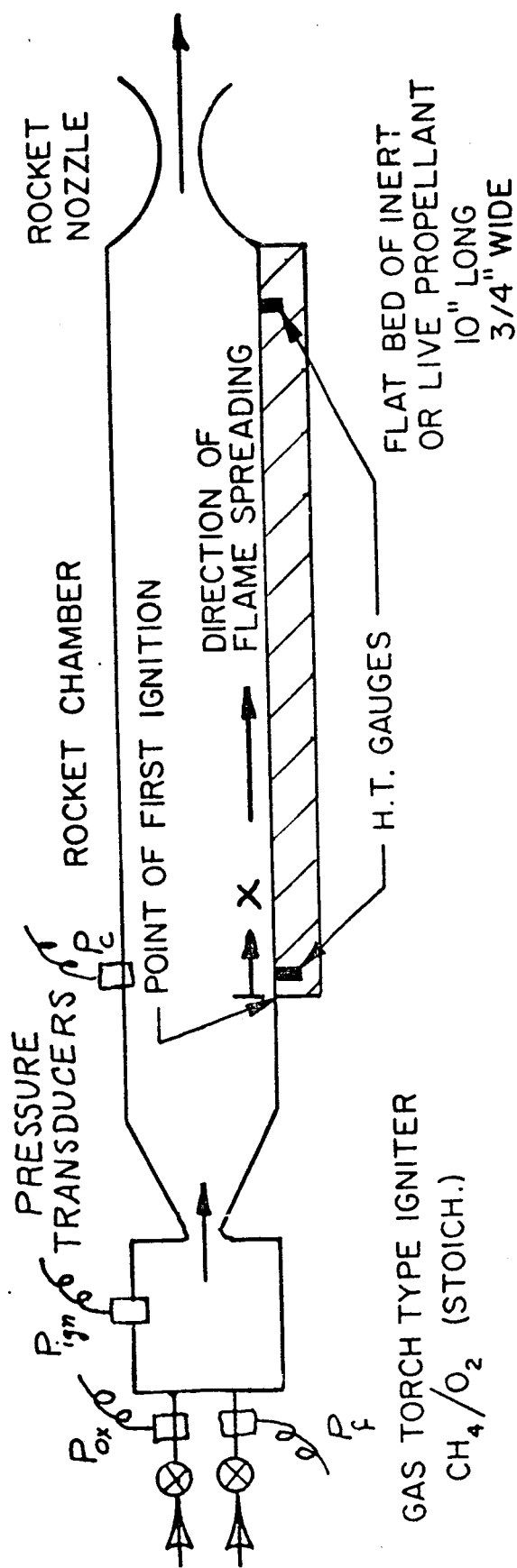
$\tau = 2.39 \text{ L}^*/\text{C}^* = 17.3 \text{ MSEC}$

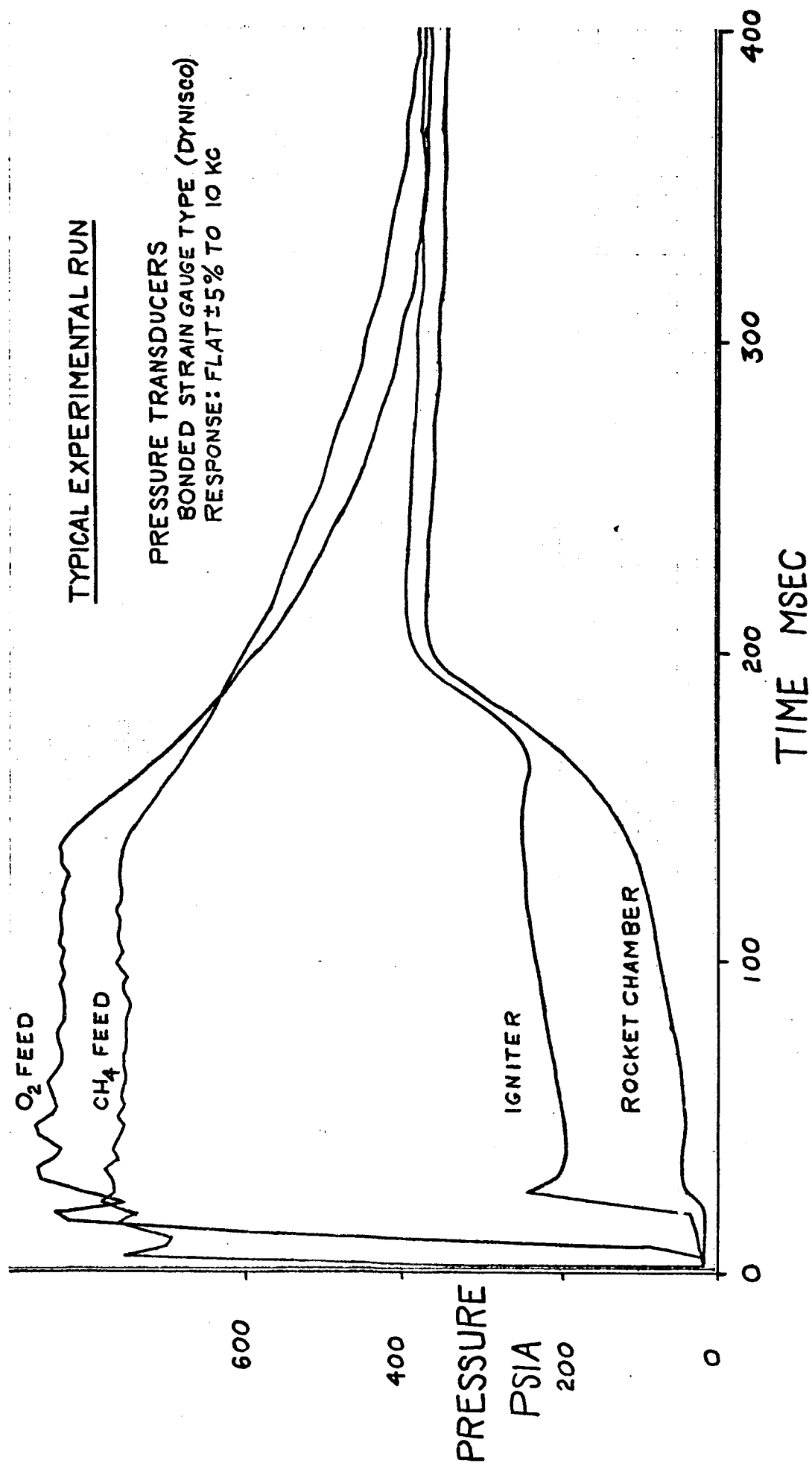
$P_{eq} = 600 \text{ PSIA}$

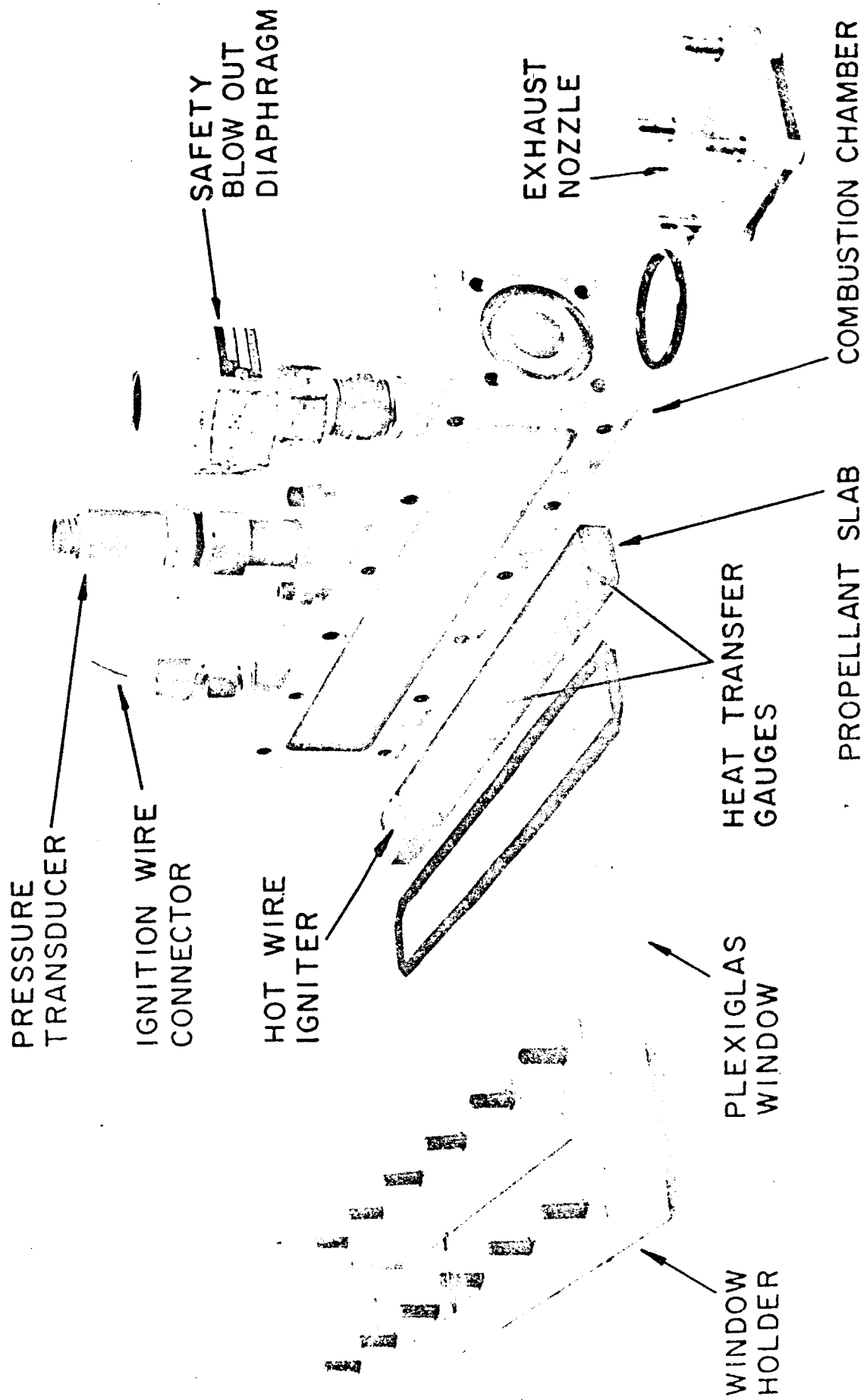
$A_p/A_t = 26.7$

∇ - IGNITER FLOW CUT-OFF

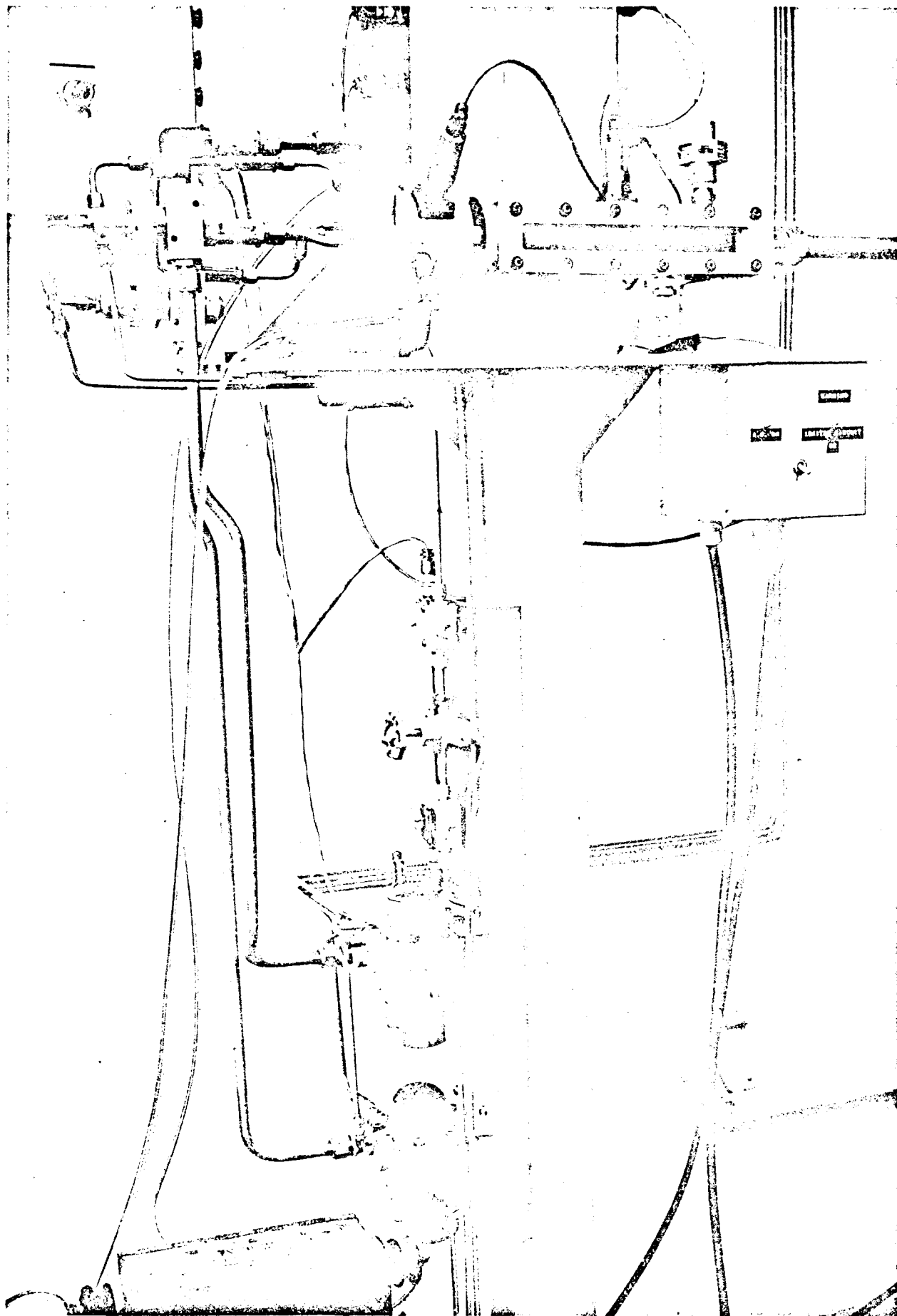




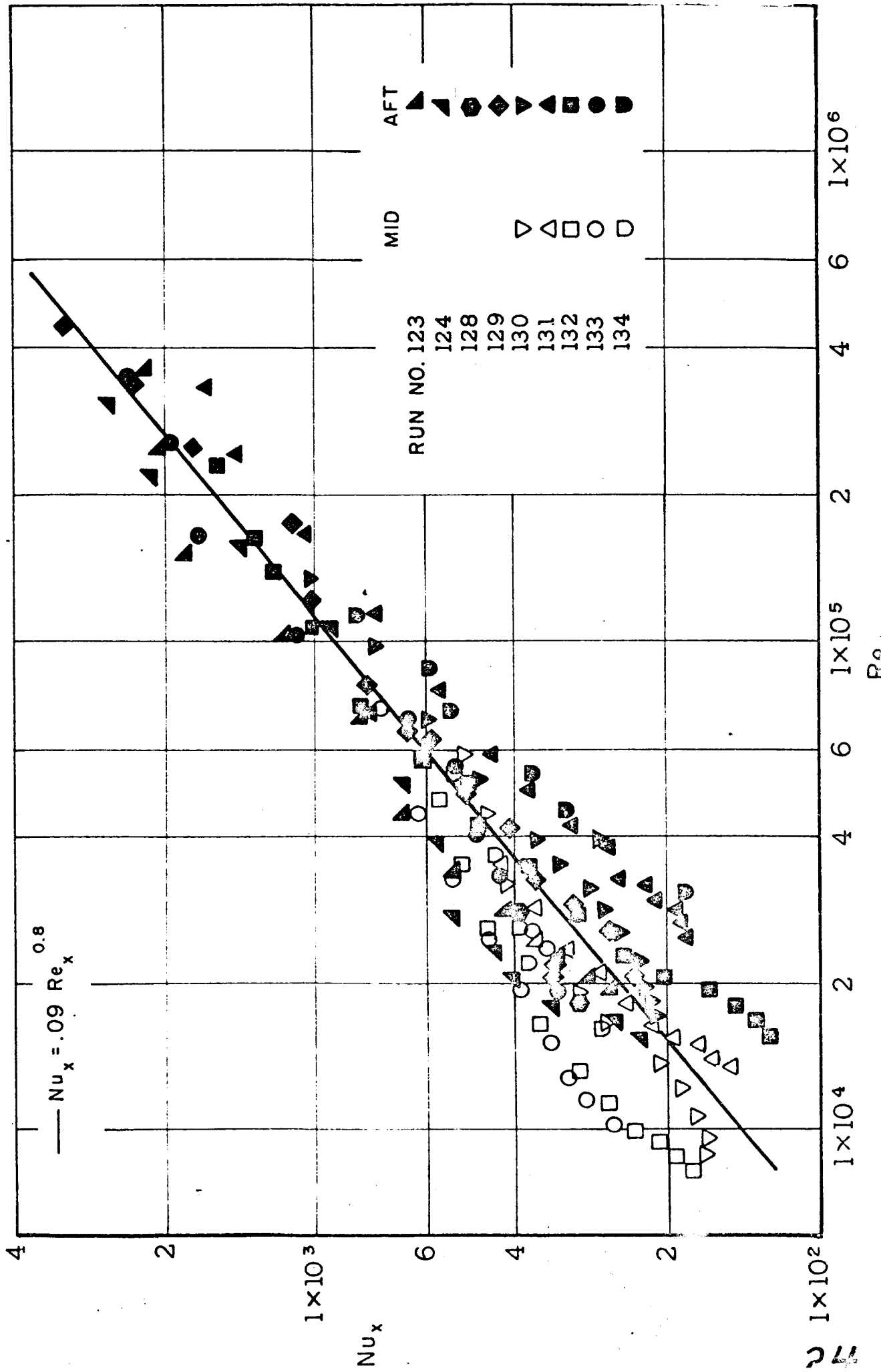


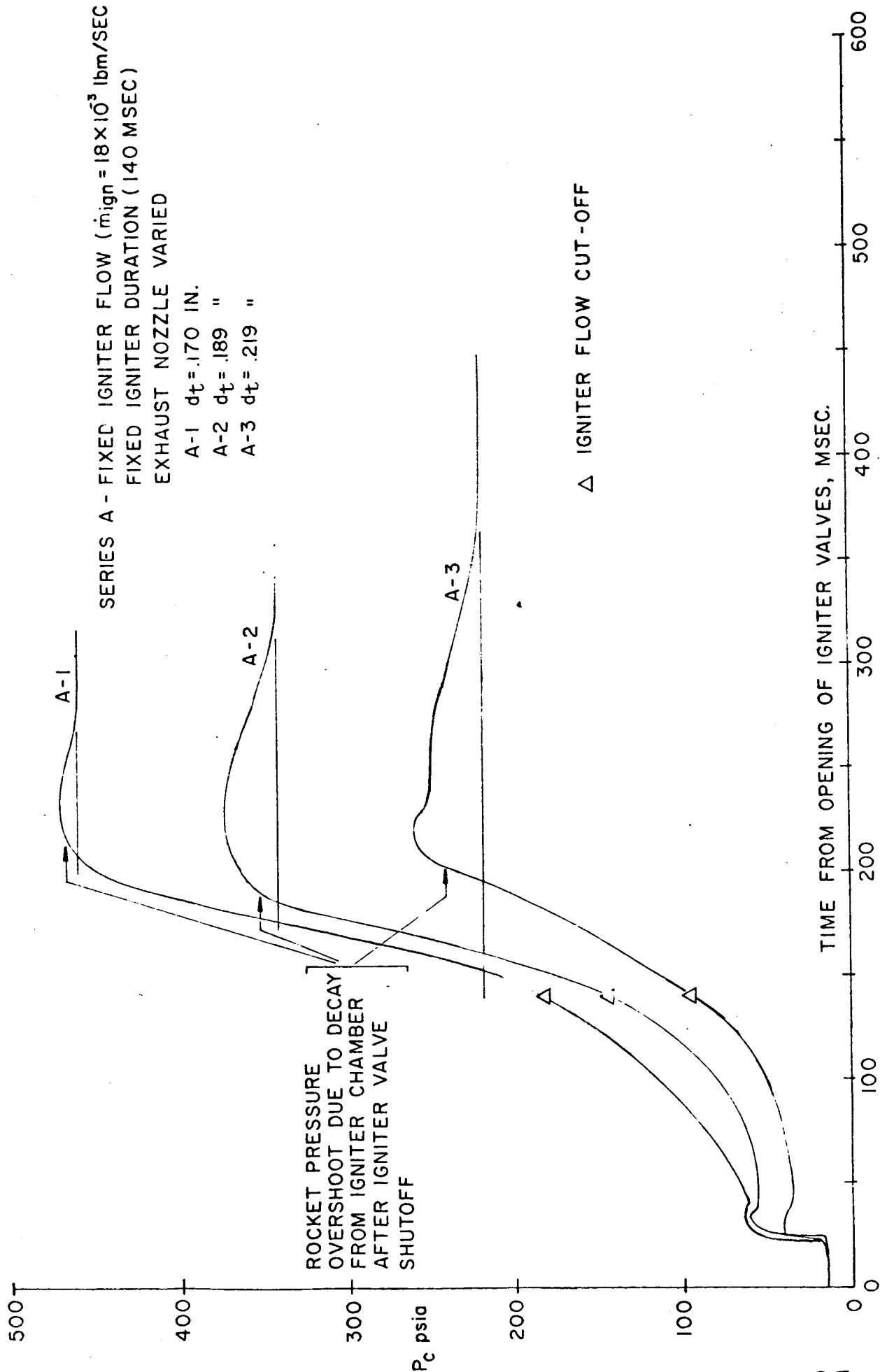


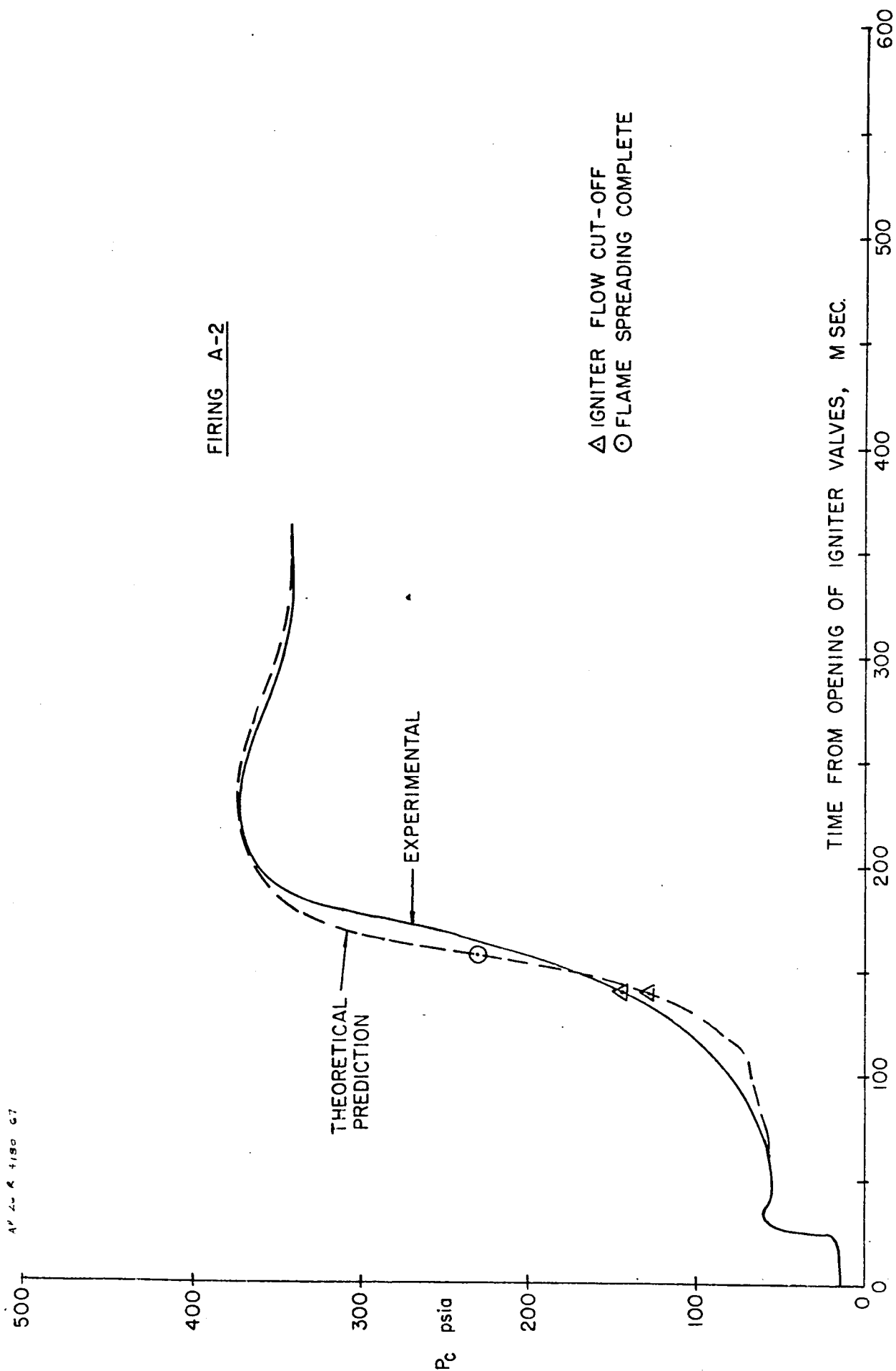
EXPERIMENTAL ROCKET MOTOR



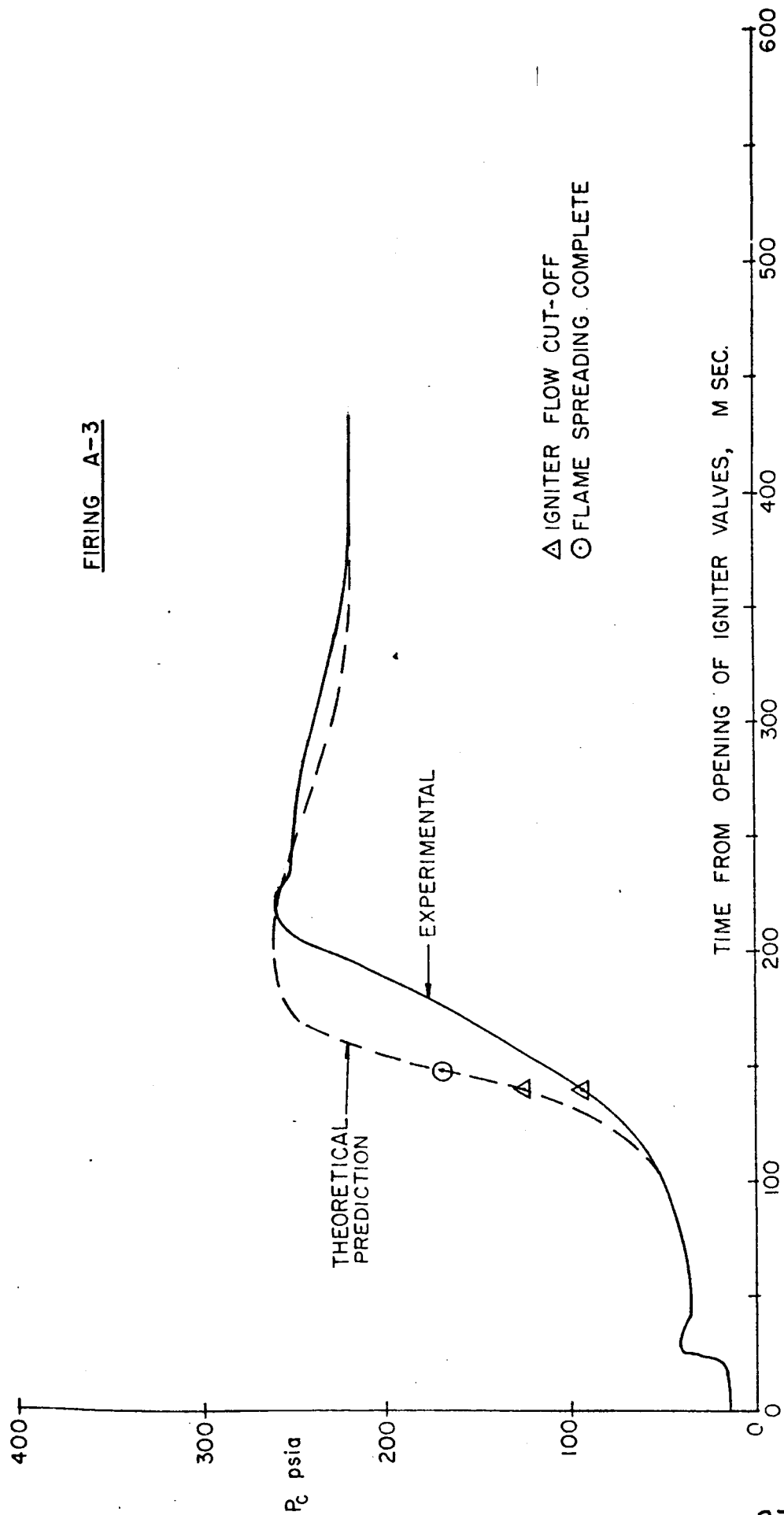
EXPERIMENTAL HEAT TRANSFER CORRELATION LOG Nu_x vs LOG Re_x







FIRING A-3



SERIES B

FIXED IGNITER FLOW ($\dot{m}_{ign} = 18 \times 10^{-3}$ lbm/SEC)

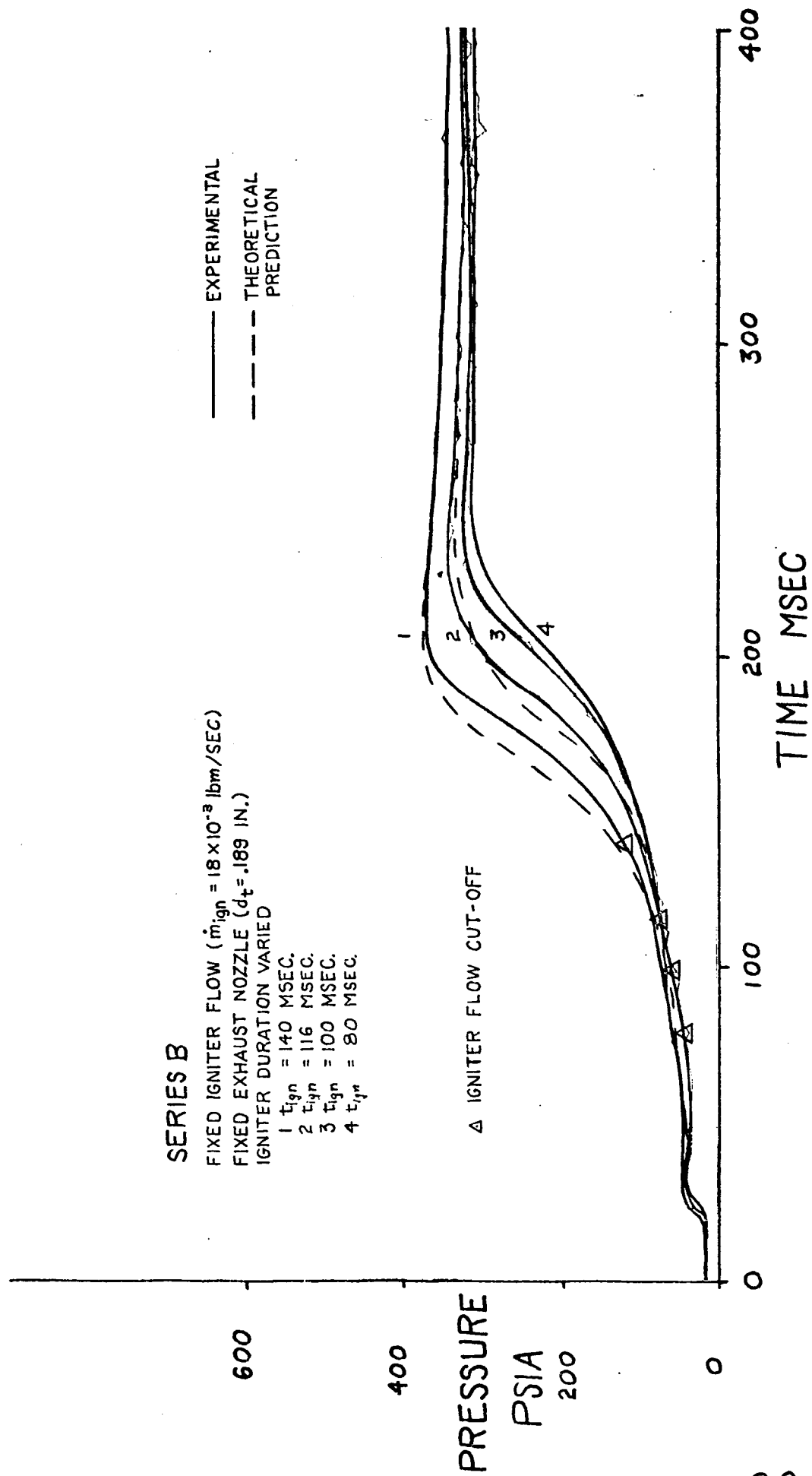
FIXED EXHAUST NOZZLE ($d_e = .189$ IN.)

IGNITER DURATION VARIED

- 1 $t_{ign} = 140$ MSEC.
- 2 $t_{ign} = 116$ MSEC.
- 3 $t_{ign} = 100$ MSEC.
- 4 $t_{ign} = 80$ MSEC.

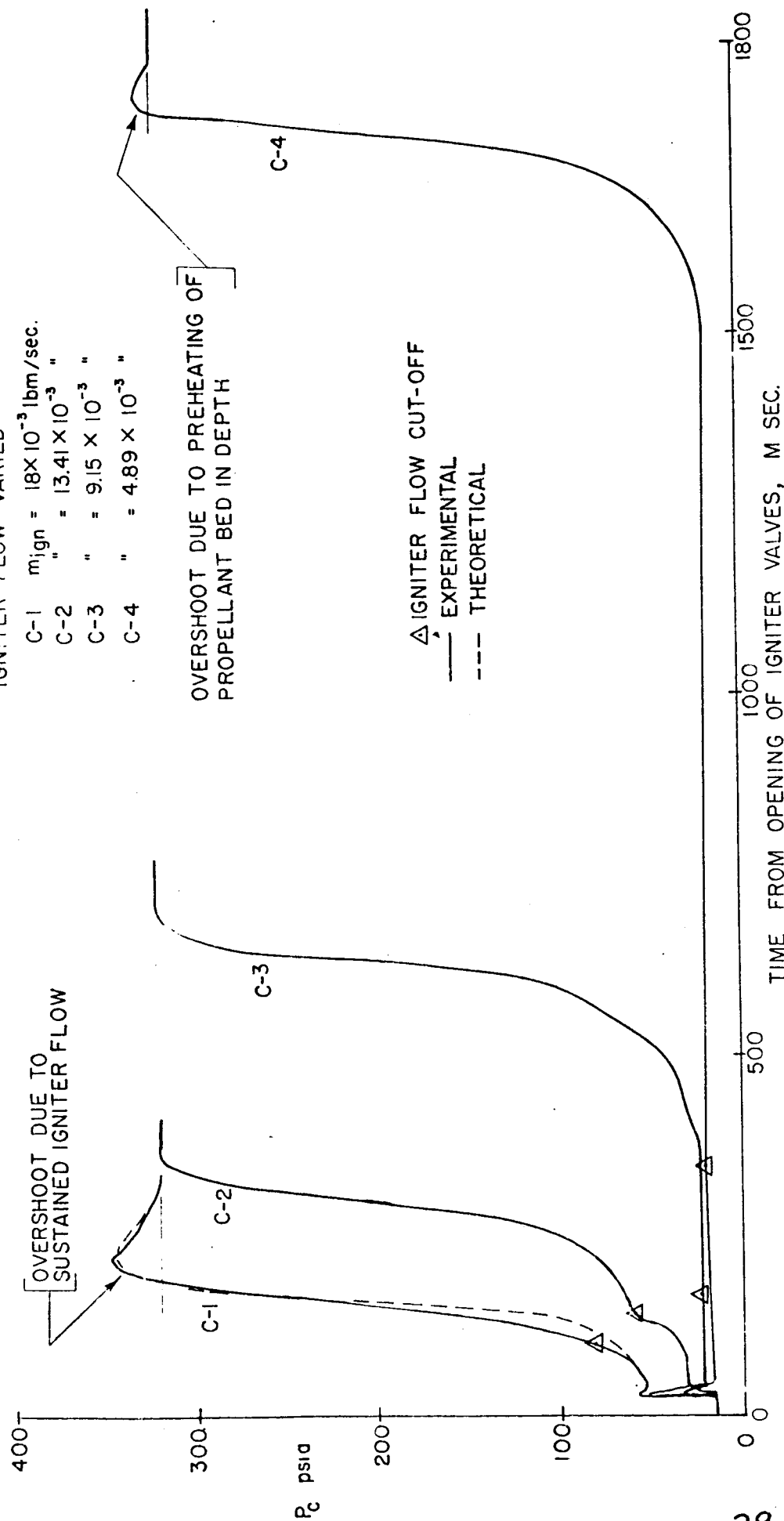
Δ IGNITER FLOW CUT-OFF

— EXPERIMENTAL
 --- THEORETICAL PREDICTION



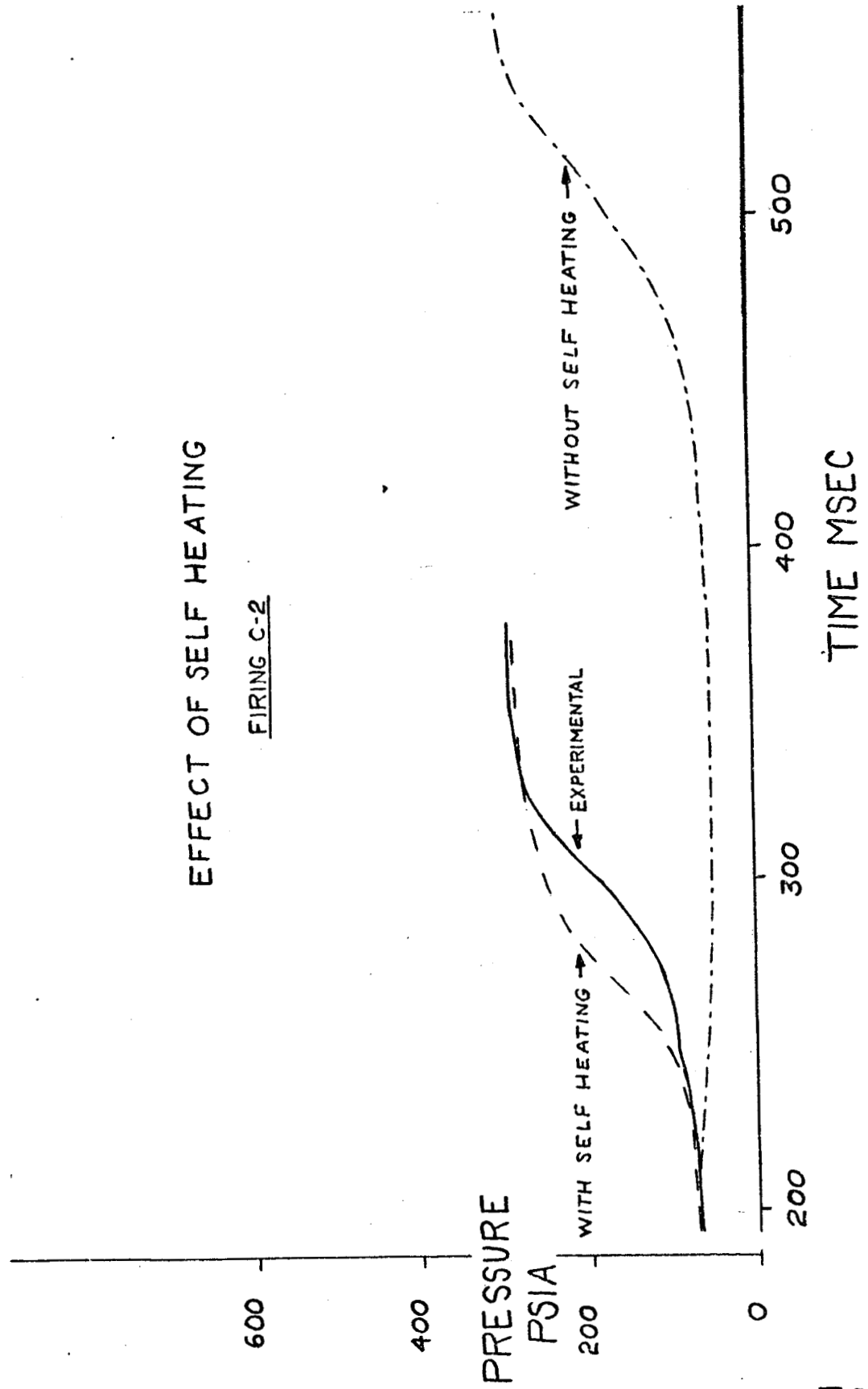
SERIES C - FIXED EXHAUST NOZZLE ($d_t = .189$ in.)
 FIXED TOTAL IGNITER/MASS $[(m_{ign})_{TOT} = 1.44 \times 10^{-3} \text{ lbm}]$
 IGNITER FLOW VARIED

C-1 $m_{ign} = 18 \times 10^{-3} \text{ lbm/sec.}$
 C-2 " $= 13.41 \times 10^{-3} "$
 C-3 " $= 9.15 \times 10^{-3} "$
 C-4 " $= 4.89 \times 10^{-3} "$



EFFECT OF SELF HEATING

FIRING C-2



Explanation of Series D

The D series of firings was intended to display the effects of varying the size of the motor exhaust nozzle systematically while other design parameters were held constant. A choice was made of the magnitude of the igniter flow and duration, and these were held constant.

This systematic variation of nozzle throat diameter, from small to large, was expected to show corresponding systematic changes in the final equilibrium pressure, from high to low. It can be seen in the following pressure-time traces of this series, that this expectation was fulfilled.

However, some irregular behavior showed up in the traces for the firings with the largest nozzles. Upon examination of this situation, it was concluded that this resulted from the choice of an igniter input (mass flow and duration) that was very close to the marginal requirement for prompt ignition. Under such circumstances, while the firings with the smaller nozzles resulted in acceptable pressure-time traces, the firings with the larger nozzles showed the erratic behavior indicative of an ignition input that is marginal.

Further verification of the interpretation that this particular choice of igniter flow and duration was marginal is provided by the appearance of some unexpected hangfires in the Series, during the test firing program. These unexpected hangfires are shown on page 32. There was no change in the firing conditions for the traces shown on page 32 as compared with the traces shown on page 31. The interpretation is clear, that the ignition exposure was marginal. As may be expected in a marginal situation, the firing behavior is sometimes normal, and in such normal situations, it was found that the experimental firing trace came close to the theoretical prediction for that situation. Such agreement is shown on the figure on page 33.

That the chosen exposure was indeed marginal was demonstrated theoretically by carrying out the computer prediction with a 10% smaller igniter mass flow than that standardized for Series D. The drastic effect of so small a reduction in the igniter mass flow is shown in the figure on page 34. The standard exposure is computed to produce a normal ignition; however, the 10% weaker exposure results in a hangfire. It is obvious that the chosen mass flow and duration were marginal for this motor.

From observation of the normal-appearing curves on page 31, it appears that enlargement of the exhaust nozzle does not stretch out the induction period but it slows down the rise

of pressure from the start of grain burning to the final equilibrium level. That the induction period is unaffected by enlargement of the exhaust nozzle follows theoretically from the fact that the heat flux in the preignition interval is not dependent on the pressure level; the slowing down of the rise of pressure after the induction interval results from the lower rate of burning associated with the enlarged exhaust nozzle.

SERIES D

FIXED IGNITER FLOW ($\dot{m}_{ign} = 18 \times 10^{-3}$ lbm/SEC)

FIXED IGNITER DURATION (60 MSEC)

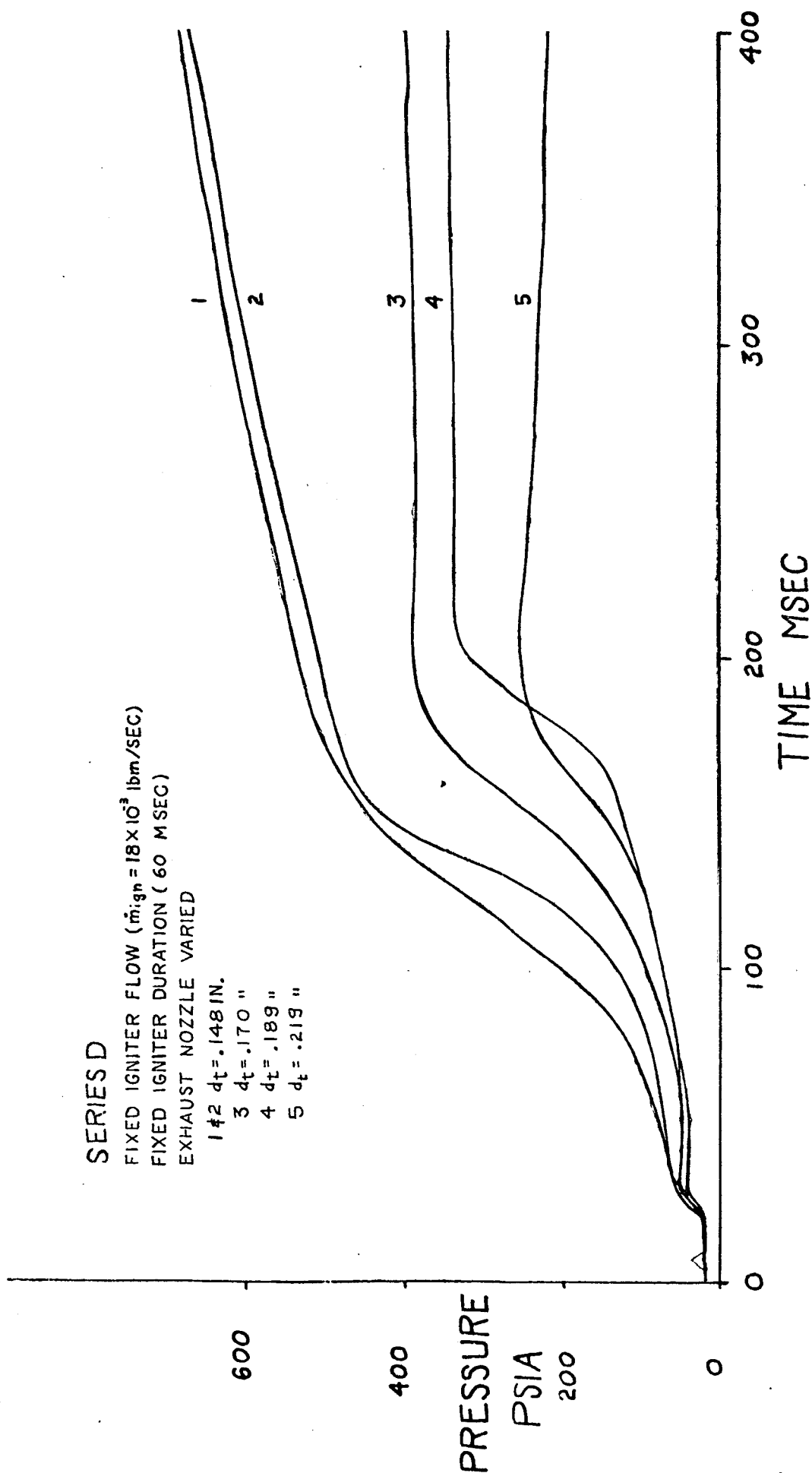
EXHAUST NOZZLE VARIED

1 #2 $d_t = .148$ IN.

3 $d_t = .170$ "

4 $d_t = .189$ "

5 $d_t = .219$ "



UNEXPECTED HANGFIRES IN SERIES D

FIXED IGNITER FLOW (\dot{m}_i ; $g^a = 18 \times 10^3 \text{ lbm/SEC}$)

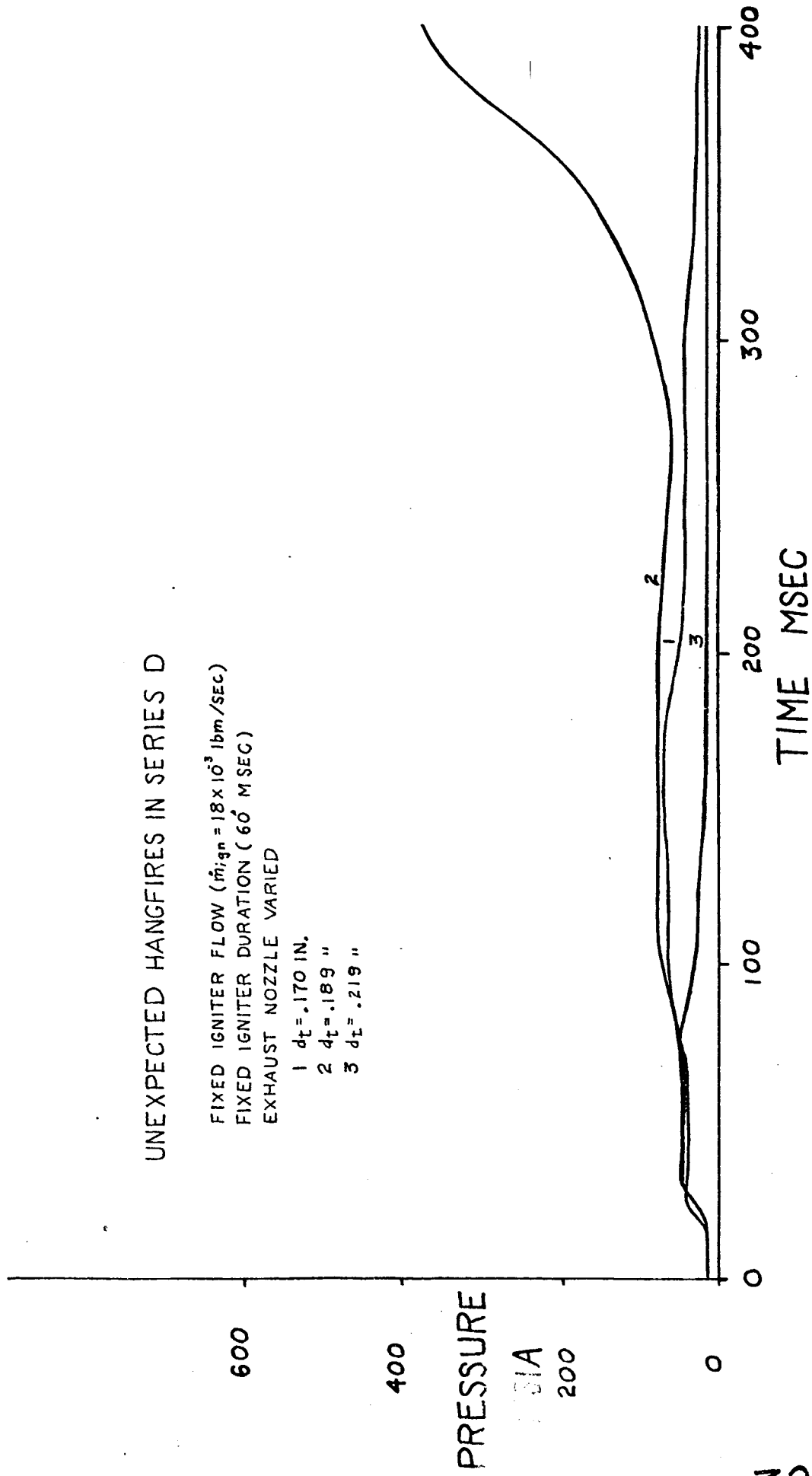
FIXED IGNITER DURATION (60 MSEC)

EXHAUST NOZZLE VARIED

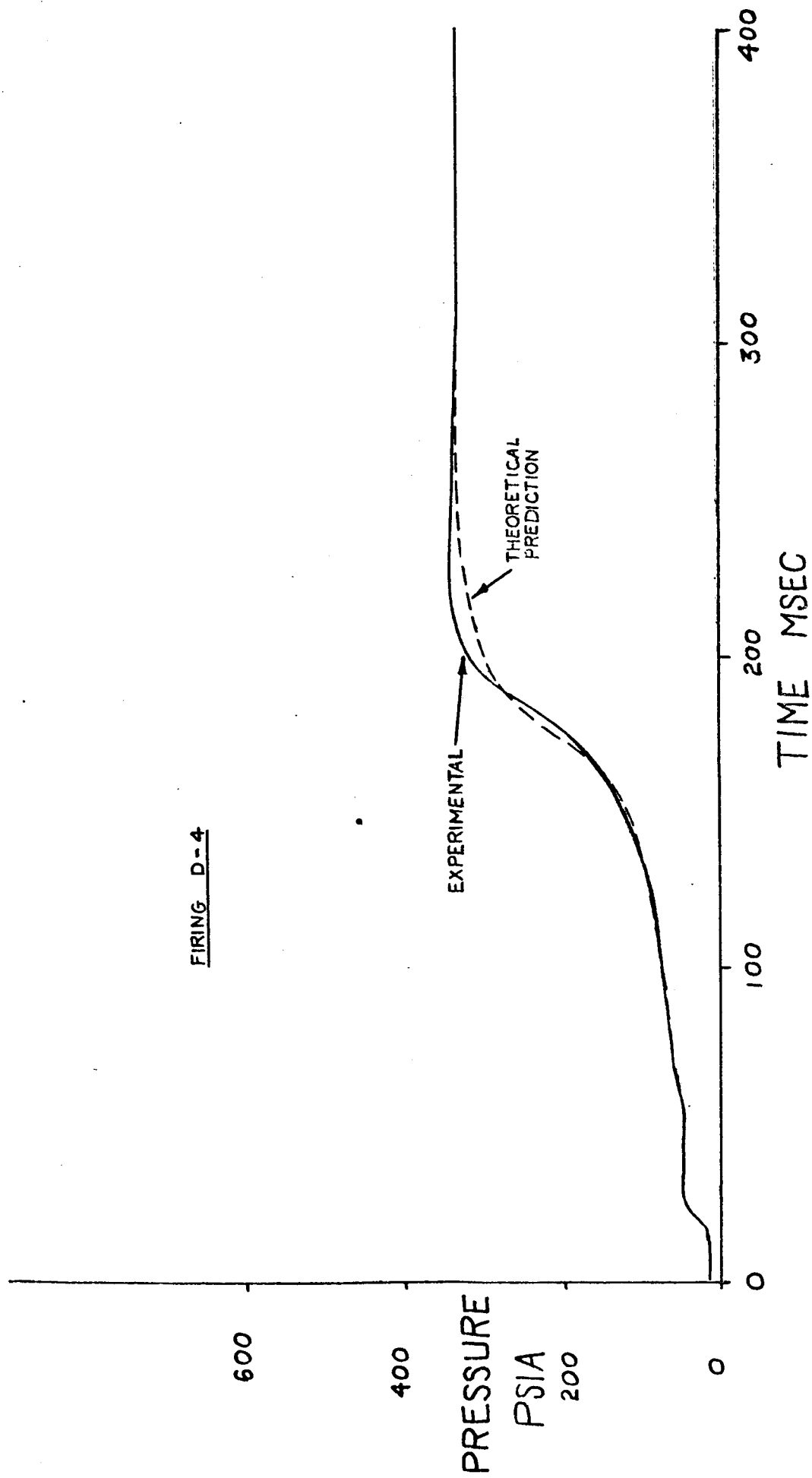
1 $d_t = .170 \text{ IN.}$

2 $d_t = .189 \text{ "}$

3 $d_t = .219 \text{ "}$

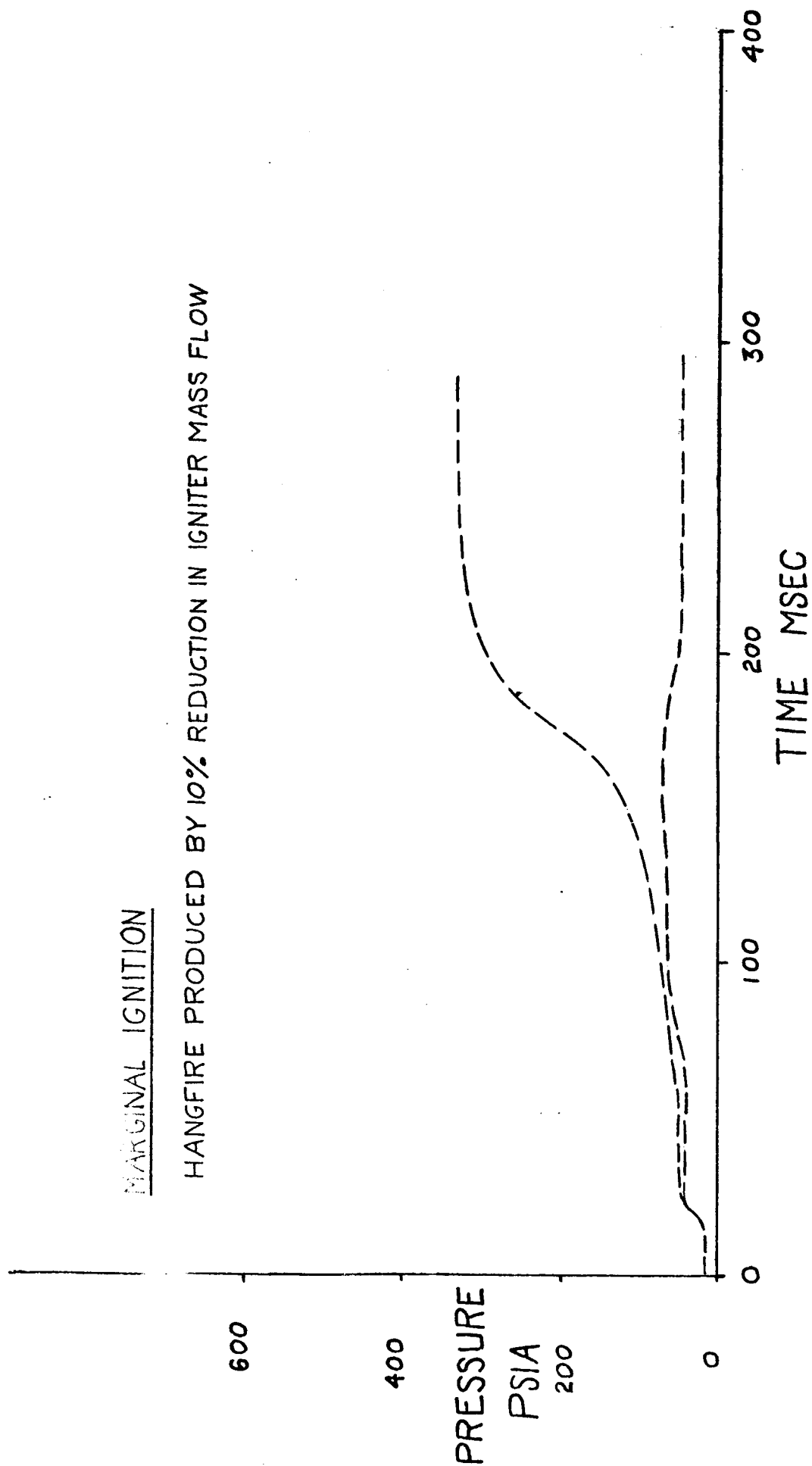


FIRING D-4



MARGINAL IGNITION

HANGFIRE PRODUCED BY 10% REDUCTION IN IGNITER MASS FLOW



Effect of Addition of Aluminum on the Ignition Transient.

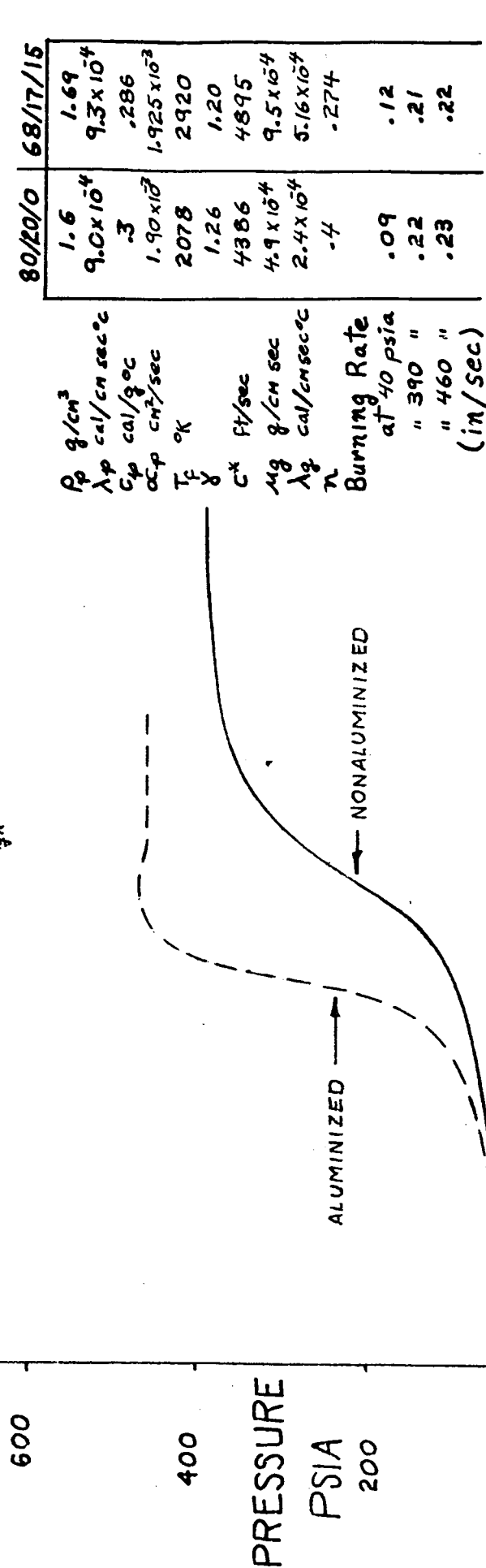
If one sets aside for the moment possible unpredictable combustion effects caused by aluminum, the presence of powdered aluminum may be expected to affect the pressure-time trace in several predictable ways. The first and most obvious is that the presence of powdered aluminum increases the thermal diffusivity of the solid propellant; this would act to slow down the rise of surface temperature at any given point on the propellant grain and thus slow down the rate of flame spreading. In addition the presence of aluminum changes both the burning rate and the pressure exponent. What these changes are depends on whether the aluminum is added at the expense of ammonium perchlorate, at the expense of fuel, or at the expense of both. For the comparative firings reported in this paper, the aluminum was added largely at the expense of the perchlorate, although some of the fuel was also removed. The percentages of the three components for the two propellants are shown at the top of the table in the figure on page 35. The burning rate exponent was depressed from 0.40 to 0.27 in the range of pressure applicable to this transient. At the same time, a significant change was observed in the burning rate of the propellant (measured in a strand burner), the value rising from 0.09 in/sec at the preignition pressure of 40 psia to 0.12 in/sec at the same pressure. Thus, the addition of aluminum made the propellant burn more actively in the lower range of pressure corresponding to the preignition interval.

In the particular firing comparison reported in this paper, the dominant factor seemed to be the increase in the burning rate at the lower level of pressure. As a result the transient became shorter. If we had been able to hold the burning rate curve unchanged, then the effect of aluminum addition would have been to delay or stretch out the ignition transient.

When the tests of aluminized propellant were extended to form Series E, (page 35) to test the effect of systematic variation of exhaust nozzle diameter, the same scatter observed in Series D (see page 31A) occurred in this Series. Some of the firing traces came out normal, and from these the effect of aluminum addition was deduced. However, for the enlarged nozzles leading to marginal ignition situations, considerable scatter was encountered, but it was not until after the entire test series was completed that it was realized that this scatter had nothing to do with the aluminization of the propellant but rather with the particular choice of a marginal ignition exposure. The interpretation of the set of curves on page 35 is the same, therefore, as for the set on page 31.

THEORETICAL PREDICTIONS FOR ALUMINIZED AND NONALUMINIZED PROPELLANT

- GEOMETRY HELD CONSTANT ($d_c = 0.2$ IN)
- IGNITER HELD CONSTANT ($t_{ign} = 135$ MSEC)



ALUMINIZED PROPELLANT SERIES E

FIXED IGNITER FLOW ($\dot{m}_{ign} = 18 \times 10^3 \text{ lbm/SEC}$)

FIXED IGNITER DURATION (60 MSEC)

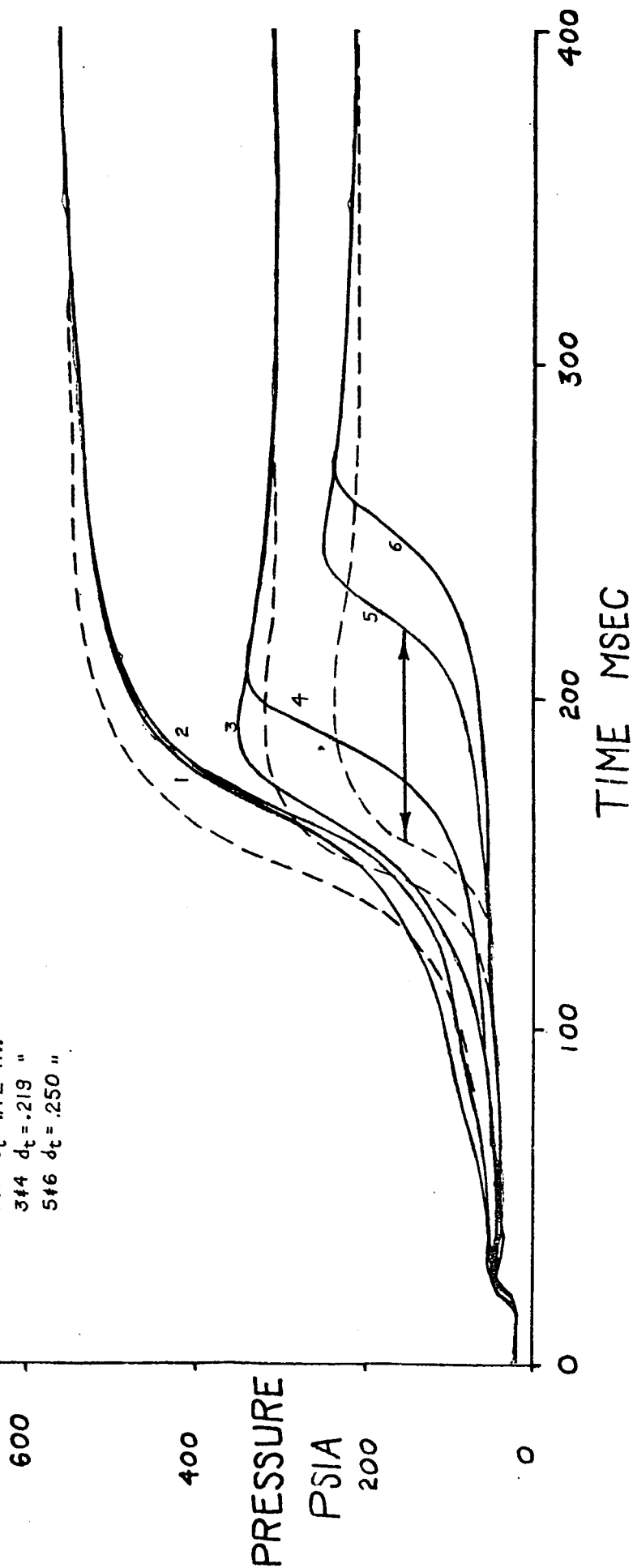
EXHAUST NOZZLE VARIED

1#2 $d_t = .172 \text{ IN.}$

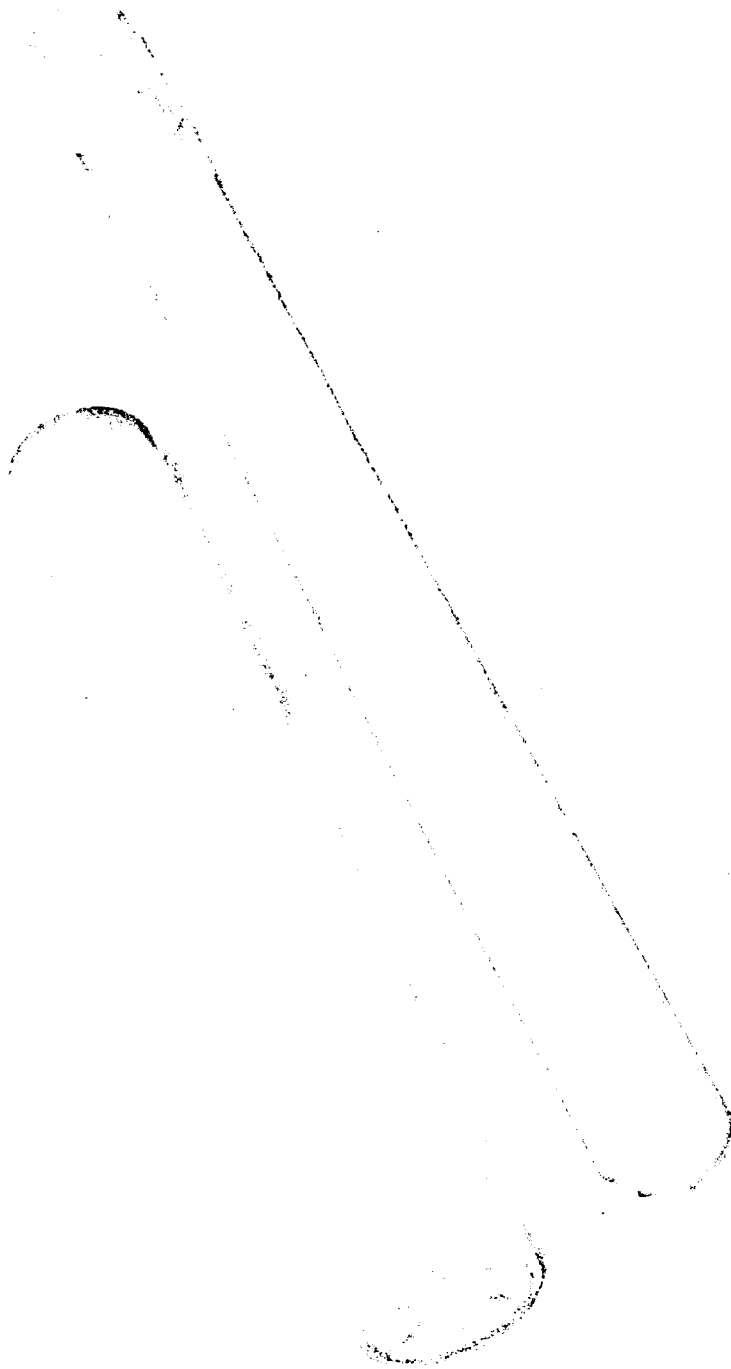
3#4 $d_t = .219 \text{ "}$

5#6 $d_t = .250 \text{ "}$

— EXPERIMENTAL
- - - THEORETICAL PREDICTION

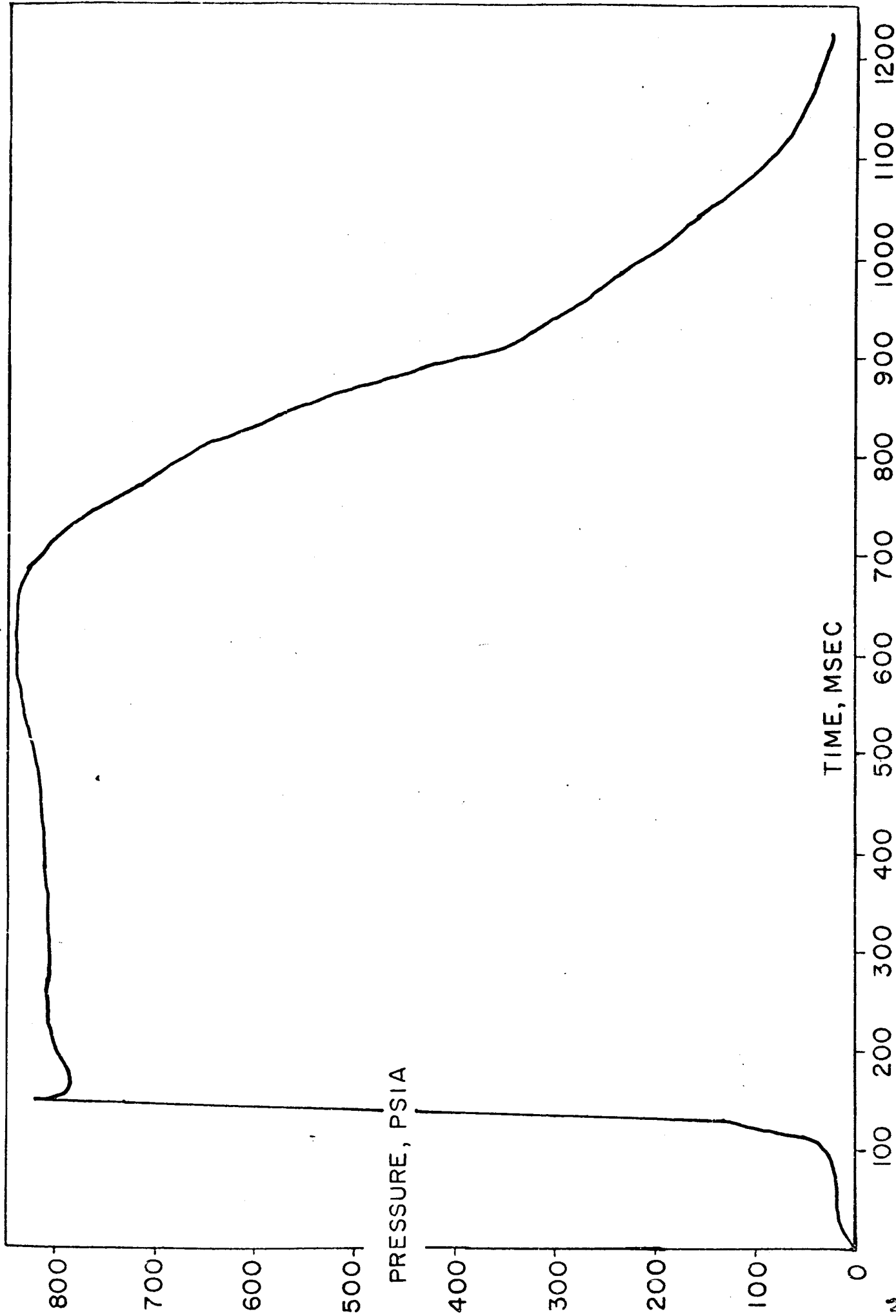


AP-26 P-15 67



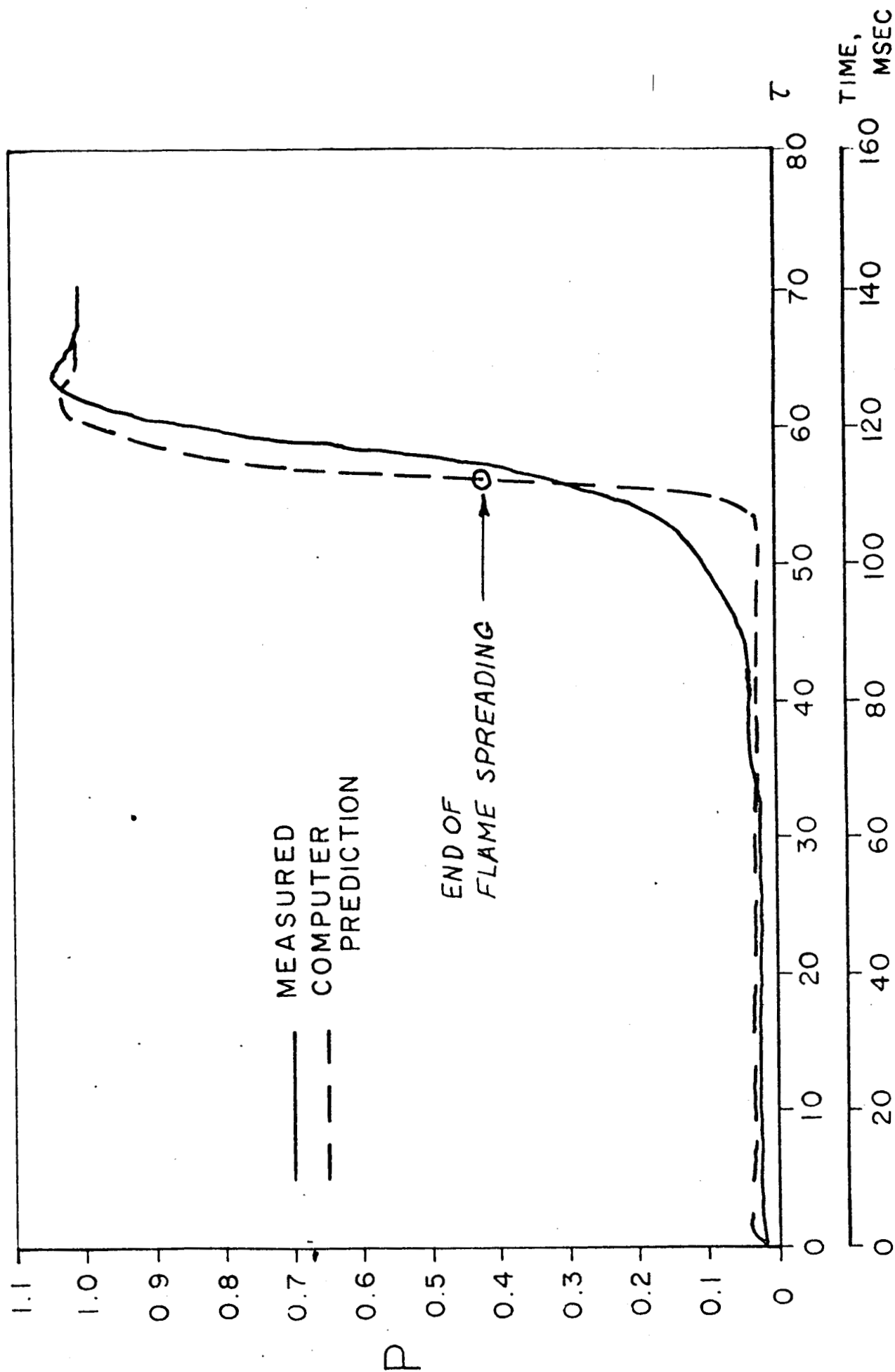
STAR SHAPE GRAIN AND MANDREL FOR EXPERIMENTAL ROCKET MOTOR

HP-26 R4113 67



TYPICAL CHAMBER PRESSURE TRACE FOR EXPERIMENTAL STAR SHAPE GRAIN

SOLID PROPELLANT ROCKET MOTOR RUN NO 84



COMPARISON OF COMPUTER PREDICTION AND MEASURED PRESSURE
TRACE FOR A TYPICAL STAR SHAPE GRAIN ROCKET MOTOR; RUN NO. 84

In conclusion, we have shown that:

1. We have developed a physically rational theory that can predict starting motor transients for motors with head-end pyrogen igniters.
2. The complete transient is predictable, including the flame spreading interval.
3. A marginal igniter can lead to a hangfire, and the boundary between a satisfactory igniter and an unsatisfactory one is very narrow.

Continued on next page.

4. Addition of aluminum powder to a propellant acts to slow down the ignition transient by increasing the thermal diffusivity. However, since the addition of aluminum changes the burning rate this prediction may be altered.
5. Pressure overshoots can be caused either by too vigorous an igniter or by a slow, long-duration igniter [pre-heating of the propellant surface.]
6. Extensions are needed in the analytical prediction method to take care of back-end ignition configurations, small port-to-throat designs, etc.

FUTURE EXTENSIONS OF THEORY

1. Small port-to-throat area ratios (high volumetric loading).
2. Gas-less igniters and igniters with intense radiation.
3. Multi-perforated grains.
4. Aft end ignition and flame spreading into stagnant regions.
5. Nonsteady state burning rate effects for very rapid transients.
6. Erosive burning effects.
7. Self heating in marginal ignition situations.

APPENDIX A

The following material is taken from a movie
which was part of the paper presentation.

THE IGNITION TRANSIENT OF
A SOLID PROPELLANT MOTOR

An Experimental Study Showing
Test Firings of a Laboratory Rocket Motor

M. Summerfield, Professor of Aerospace Propulsion

P. L. Stang, Member of Professional Staff

W. J. Most, Ph.D. Candidate

B. W. MacDonald, Undergraduate (Junior)

C. R. Felsheim, Engineering Specialist

S. O. Morris, Lead Technician

E. R. Crosby, Lead Technician

Department of Aerospace & Mechanical Sciences

Princeton University

Prepared for Presentation at
The Third ICRPG/AIAA Solid Propulsion Conference
Atlantic City, New Jersey
June 4-6, 1968

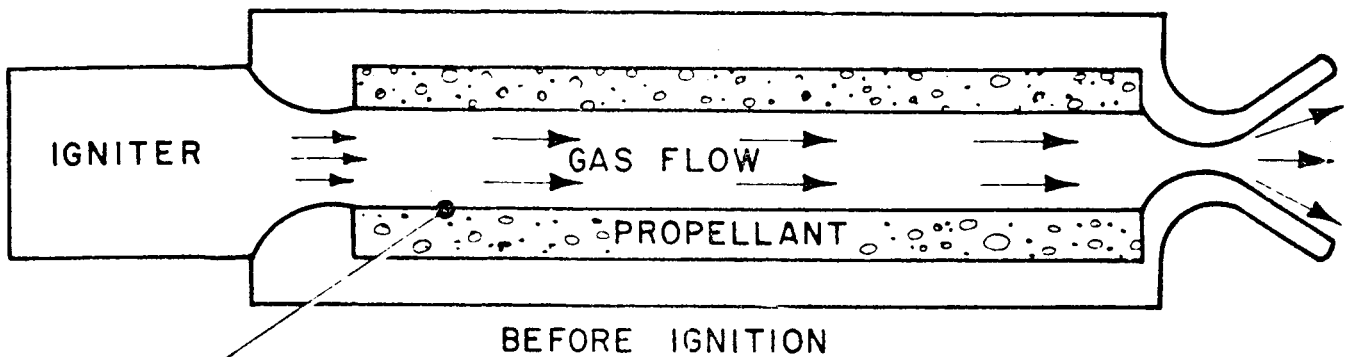
A basic research program sponsored by
The National Aeronautics and Space Administration
under Grant NGR 31-001-109 and
supervised by the Langley Research Center

INTRODUCTION

The ignition transient can be divided into three distinct intervals:

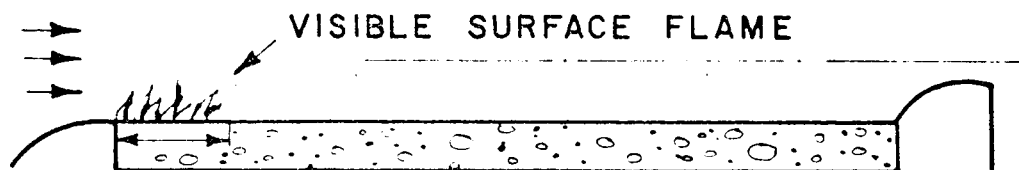
1. Induction Interval - The time from the first application of the igniter stimulus to the exposed surface of the grain until the appearance of the first flame.
2. Flame Spreading Interval - The time from the appearance of the first flame until the entire propellant grain is burning.
3. Chamber Filling Interval - The time from the end of flame spreading until the equilibrium pressure is attained.

SCHEMATIC REPRESENTATION, FLAME SPREADING PHASE OF IGNITION INTERVAL

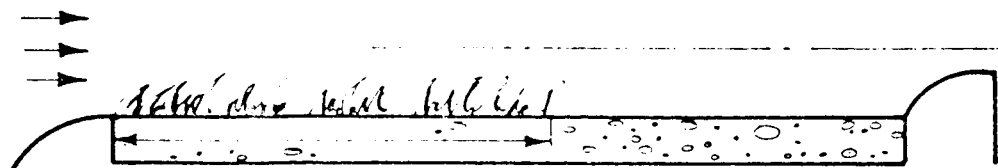


SUCCESSIVE POSITIONS OF SURFACE FLAME
AFTER START OF IGNITION

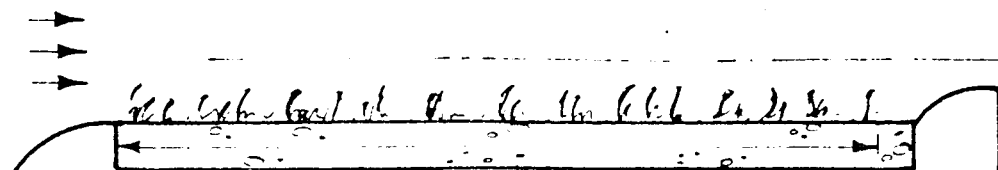
▼
A - FIRST
VISIBLE
FLAME



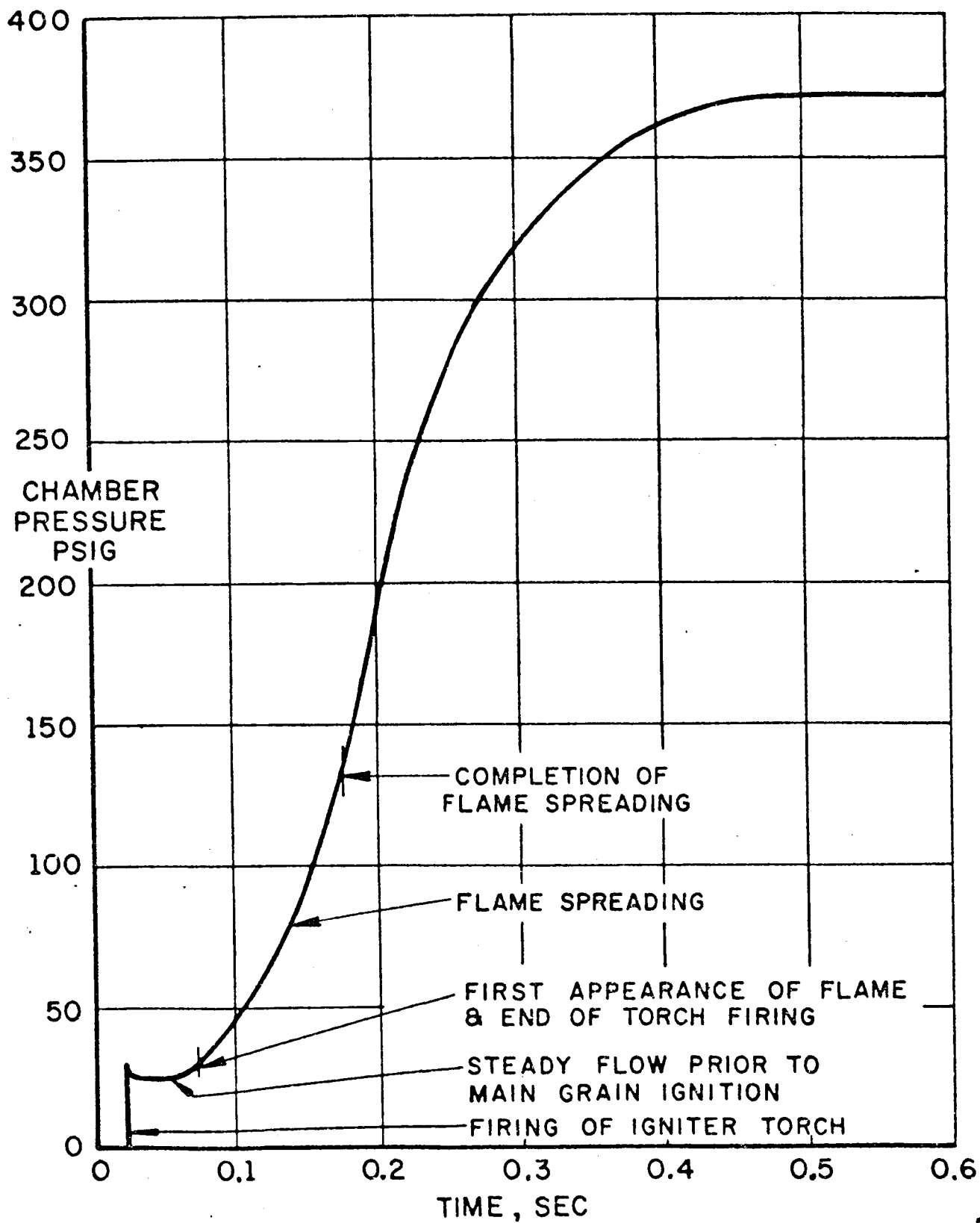
B - INTERMEDIATE
STAGE



C - ALMOST
FULLY
IGNITED



PRESSURE TRANSIENT DURING IGNITION OF TEST MOTOR



This film deals with the flame spreading intervals for three situations of particular interest:

1. Flame spreading over an unaluminized propellant grain.
2. Flame spreading over an aluminized propellant grain.
3. Flame spreading during a hangfire.

First, some description of the laboratory motor and pyrogen-type igniter ---

EXPERIMENTAL MOTOR

The experimental motor was approximately square in cross-section ($1" \times 3/4"$). One side wall had a Plexiglas window permitting photographic observation of the flame inside the chamber. The typical nozzle throat was $1/4$ inch in diameter. The chamber pressure ranged from about 100 to 800 psia. The typical thrust level was about 15 lbs.

IGNITER

Ignition was achieved with the hot gases from a methane-oxygen combustor fitted to the forward end of the rocket motor, which in turn was started by fast action valves and ignited by a spark. The temperature of the hot igniter gas was estimated to be 2500°K . The igniter mass flow rate was set at about 0.018 lbm/sec, which established pre-ignition pressures in the rocket motor ranging from 30 to 90 psia, depending on the exhaust nozzle diameter.

MOVIE SCENE 1

This piece of film shows a view of the experimental motor and the pyrogen-type igniter mounted on the test stand. A view of the surrounding test cell is also shown.

PROPELLANT GRAIN

The propellant grain was a thin, flat slab 3/4 inch wide by 9 1/2 inches long, weighing about 50 grams. The propellant was a composite PBAA-Epon 828/AP type made in our own laboratories. The burning rate at 1000 psia was 0.30 in./sec and 0.13 in./sec at 100 psia. The measured ignition temperature was about 420°C.

CASE 1:

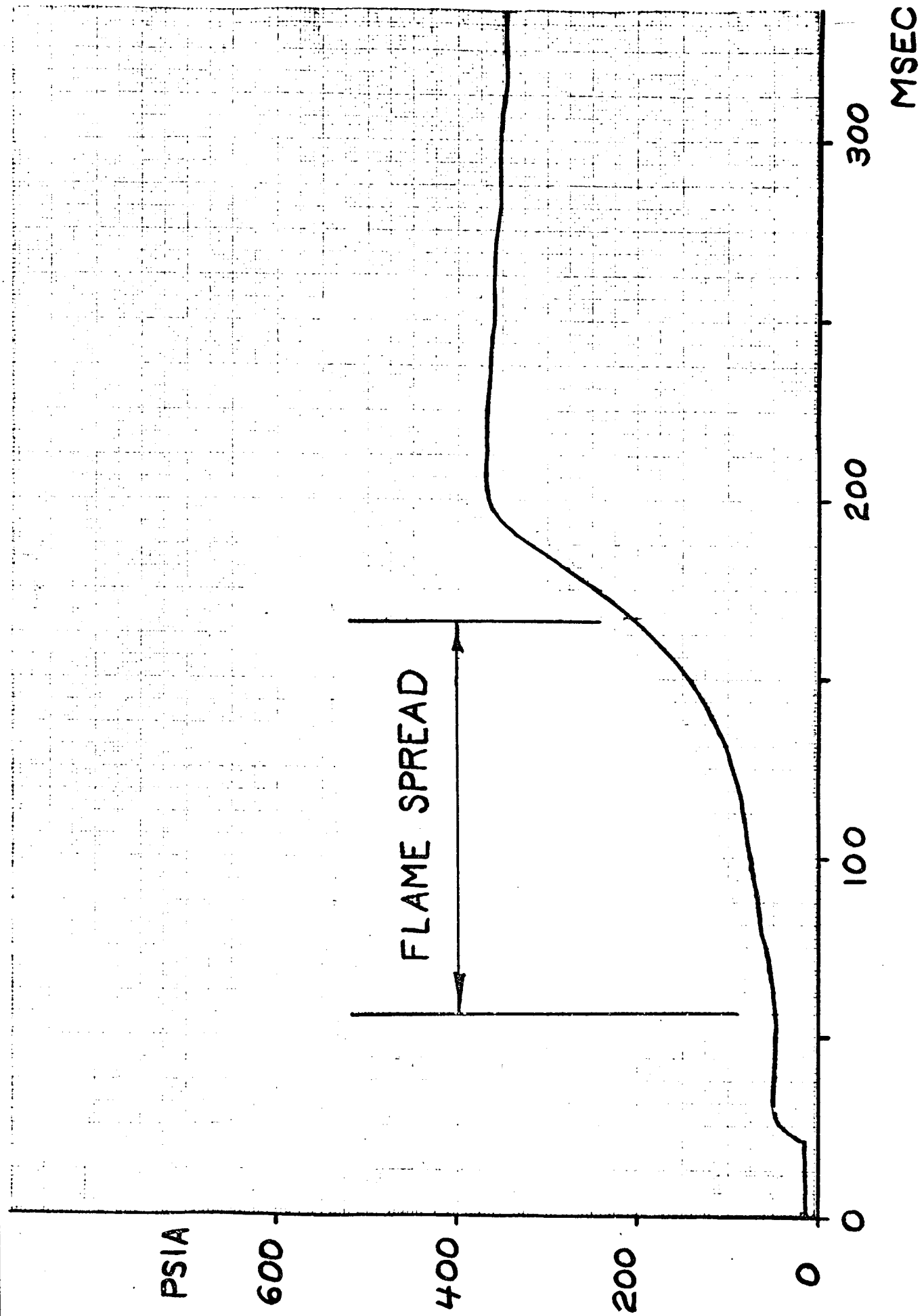
FLAME SPREADING OVER AN UNALUMINIZED PROPELLANT

Propellant: PBAA(20%)/AP(80%)

You will see a view of the test rocket motor showing the window through which the propellant flame will be seen. After viewing the motor, the illumination will go out and then the igniter will start. After a short time (an induction interval of about 40 msec), the leading edge of the propellant grain will start to burn. Flame spreading will then ensue, running from left to right. (framing rate: 2000 frames/sec)

MOVIE SCENE 2

This piece of film shows a close-up view of the experimental motor showing the observation window. The flame spreading over an unaluminized propellant grain is then seen.



WHAT YOU SAW IN THE FIRING TEST

After an induction period (not all of it was shown) in which no flame was seen on the propellant, you saw ignition take place at the leading edge. As the flame advanced to the right (toward the exit nozzle), bits of flame appear at isolated spots ahead of the main flame front. These flamelets did not spread (theory says they should not) and they eventually were overtaken by the main flame.

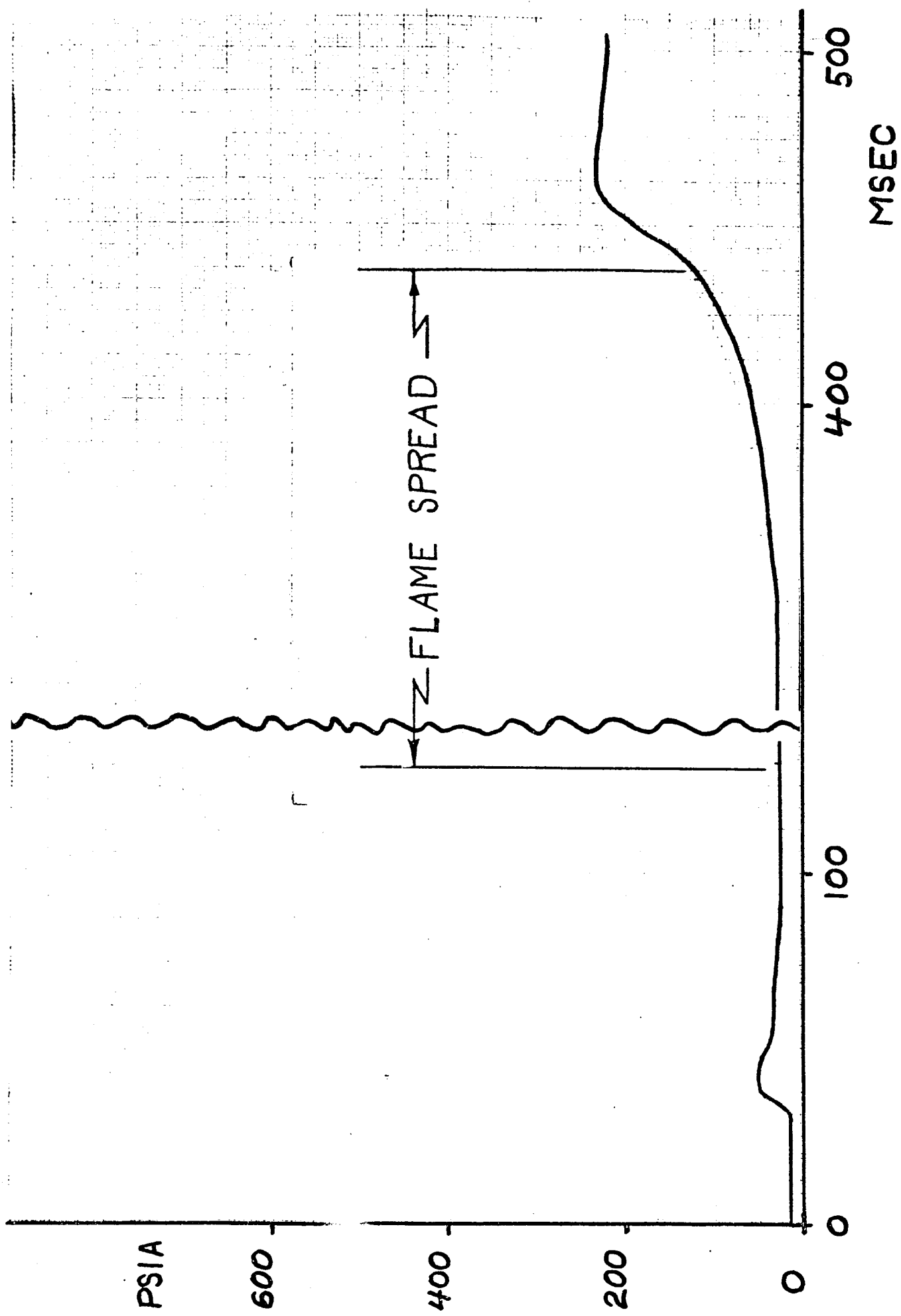
CASE 2:

FLAME SPREADING OVER AN ALUMINIZED PROPELLANT

Propellant: PBAA(17%)/AP(68%)/Al(15%)

THE IMPORTANT FEATURES TO BE OBSERVED ARE:

1. Particles of molten aluminum can be seen rising from the ignited portion of the grain and entering the main gas stream. Many are seen rolling down the surface.
2. In general, those particles that hit the unignited surface do not attach themselves there or cause any significant spread of ignition as they travel downstream.
3. In short, the flame spreading over aluminized propellant is very similar to flame spreading over unaluminized propellant. The quantity of hot aluminum particles liberated from the grain are not sufficient to augment significantly the spread of ignitedness.



MOVIE SCENE 3

This piece of film shows the flame spreading
over an aluminized propellant grain.

CASE 3:

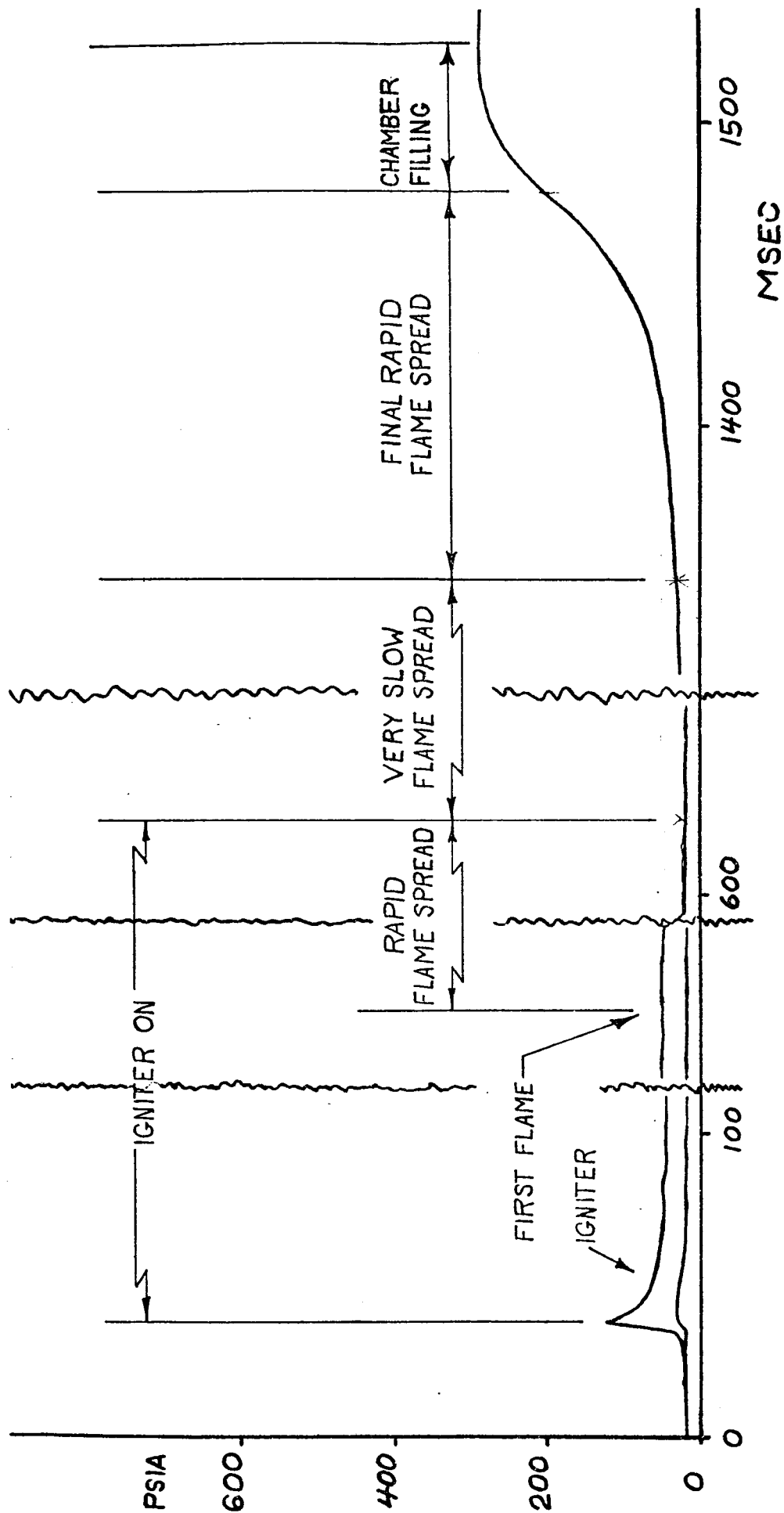
FLAME SPREADING DURING A HANGFIRE

When the igniter heat stimulus is stopped too soon after the start, so that the small portion of the propellant grain then burning generates insufficient hot gas to carry out rapid completion of flame spreading, a hangfire will occur.

Propellant: PBAA(20%)/AP(80%)

THE IMPORTANT FEATURES TO BE OBSERVED ARE:

1. Rapid flame spreading occurs right after the appearance of the first flame and continues until approximately 25% of the grain is ignited.
2. The flame spreading rate is markedly reduced, nearly to zero, right after the igniter stimulus is removed.
3. Finally, after a long delay, rapid flame spreading takes place over the remainder of the grain.



MOVIE SCENE 4

This piece of film shows the flame spreading over an unaluminized propellant grain during a hangfire situation.